THE UNIVERSITY OF MICHIGAN
COLLEGE OF ENGINEERING
Department of Nuclear Engineering

Technical Report

STUDY OF LITHIUM MOBILITY IN IRRADIATED SILICON

Walter A. Hackler
Chihiro Kikuchi

ORA Project 04381

supported by:

NATIONAL AERONAUTICS AND SPACE ADMINISTRATION
GRANT NO. NsG-115-61
WASHINGTON, D.C.

administered through:

OFFICE OF RESEARCH ADMINISTRATION ANN ARBOR

July 1966

This report was also a dissertation submitted by the first author in partial fulfillment of the requirements for the degree of Doctor of Philosophy in The University of Michigan, 1966.

TABLE OF CONTENTS

	Page
LIST OF TABLES	iv
LIST OF FIGURES	v
ABSTRACT	vii
Chapter	
I. INTRODUCTION	1
II. GENERAL THEORY	7
A. Ionization of Impurities in Semiconductors	
B. Ion Pairing	
C. Lithium-Vacancy Precipitation	
D. Determination of Lithium Ion Mobility	
III. EXPERIMENTAL PROCEDURE	37
A. Diode Preparation	
B. Neutron Irradiation	
C. Electron Irradiation	
D. Gamma Irradiation	
E. Lithium Drift and Diode Capacitance Measurement	
IV. ANALYSIS AND DISCUSSION OF RESULTS	46
A. Determination of Lithium Mobility in Boron Doped Silicon	
B. Lithium Mobility in Neutron Irradiated Silicon	
C. Lithium Mobility in Electron Bombarded Silicon	
D. Analysis of the Lithium-Vacancy Precipitate	
V. CONCLUSIONS	75
APPENDICES	80
A. Quantitative Description of the Semiconductor Water Analogy	
B. Sample Calculations	
BIBLIOGRAPHY	86

LIST OF TABLES

Table		Page
1.	Lithium Diffusion Coefficient in Neutron Irradiated Silicon	56
2.	Lithium Diffusion Coefficient in Electron Bombarded Silicon	61
3.	Calculations for the Ion Pair Model: $\frac{P/N}{(1 - P/N)^2} = N_E E^{K_p}$	65
4.	Calculations for Lithium-Vacancy Precipitation: $(1-S/N) = K_s'/ N_E$	69
5.	Lithium Diffusion Coefficient in Irradiated Silicon	76
6.	Comparison of Silicon and Germanium to Water	82

LIST OF FIGURES

Figure		Page
1.	An Energy Band Diagram for Silicon Showing the Equilibrium Relations (1), (2) and (3)	13
2.	Equilibrium Distribution of Lithium Nearest Neighbors About a Boron Ion	19
3.	Lithium Distribution (N_{Li}) in Silicon After an Initial Diffusion Period t_o	28
4.	Lithium Distribution (N_{Li}) in Silicon After a Period of Ion Drifting, t	30
5.	A Tube Diffusion Furnace	38
6.	Dicing the Wafer Diode	40
7.	A Prepared Lithium Diffused Diode	40
8.	Electron Bombardment of the Diced Diode	43
9.	Jig Designed to Hold Several Diodes in a Constant Temperature Bath	43
10.	Effect of Boron Concentration on Lithium Diffusion Coefficient in Silicon	48
11.	$(10^3/C)^2$ Versus Drift Time for Neutron Irradiated Silicon Diodes	49
12.	$(10^3/C)^2$ Versus Drift Time for Annealed Neutron Irradiated Samples	52
13.	Relative Effect of Thermal and Epithermal Neutrons on Lithium Drift in Silicon	53
14.	Effect of Fast Neutron Bombardment on the Diffusion Coefficient of Lithium in Silicon	57
15.	$(10^3/C)^2$ Versus Drift Time for Electron Bombarded Diodes .	58

Figure Page

16. $(10^3/C)^2$ Versus Drift Time for Electron Bombarded Diodes . 59

17. Effect of Electron Bombardment on the Lithium Diffusion Coefficient in Silicon 60

18. A Plot of $\frac{P/N}{(1 - P/N)}^2$ Versus N_E 64

19. A Plot of $(1 - S/N)$ Versus $1/N_E$ 68

20. A Plot of $(1 - S/N)$ Versus $1/N_E$ or $1/N_N$ for All Data . . . 70

Abstract

The objective of this study is to determine experimentally the effect of fast neutron and electron induced defects on the diffusion properties of lithium in silicon. The effect was determined by irradiating lithium diffused diodes and subsequently applying a reverse bias to the junction at a constant temperature.

Experimental results show that fast neutron and 0.9 MeV electron induced vacancies provide sites for the precipitation of lithium. Moreover, the lithium vacancy precipitate behaves like a solute in equilibrium ions and ionized vacancies. The analysis of the lithium vacancy precipitate in this fashion is analogous to the analysis of slightly soluble salts in water.

The lithium diffusion coefficient for silicon exposed to fast neutrons, N_N = 1.1 to 2.7 x 10^{14} neutrons/cm^2, can be expressed

$$D = \frac{7.0 \times 10^{12}}{N_N} e^{-0.83/kT} \quad cm^2/sec .$$

The range of (T) in the above expression is from 300° to 410°K.

It also was shown that the motion of lithium in silicon was not affected by slow neutron irradiation.

In addition, the lithium diffusion coefficient for silicon exposed to 0.9 MeV electrons, N_E = 5 x 10^{15} to 3.3 x 10^{16} electrons/cm^2, can be represented by

$$D = \frac{2.1 \times 10^{18}}{N_E} e^{-1.03/kT} \quad cm^2/sec \quad .$$

The range of T in the above expression is from 300° to 330°K.

Relative radiation damage between neutrons and electrons was found to be in reasonable agreement with predictions based on radiation damage theory.

CHAPTER I

INTRODUCTION

Solid state detectors have become indispensable in the detection and study of nuclear radiation. Successful fabrication and operation of these detectors is dependent on the purity and quality of single crystal silicon and germanium. For junction and surface barrier detectors, the radiation sensitive thickness of the detector is directly proportional to the one half power of resistivity of the silicon or germanium. The purest n-type detector grade silicon available at present has a resistivity of 10,000 ohm-centimeter. Detectors constructed of this material are suitable for heavy charged particles, but do not have sufficient sensitive thickness to be employed in electron or gamma spectrometry.

The process of drifting lithium in silicon to produce highly compensated regions of high resistivity was developed by Pell.[1,2] With the use of lithium drifted silicon, detectors can be developed that are suitable for electron and gamma spectrometry. The drifting procedure is accomplished by the application of a reverse bias to an n-p silicon junction in which the n-side is lithium doped by diffusion, and the p-side is doped with acceptor atoms. Under the influence of the applied electric field the lithium will move (drift) from the n-side of the junction to the p-side. As it drifts the lithium will interact with the

substitutionally bound acceptor atoms and produce a region of very high compensation. The lithium drifting technique can be employed to create p-i-n detectors or provide material for surface barrier detectors.[3,4,5,6,7,8,9]

The increased sensitivity of the lithium drift detector is accompanied by greater susceptibility to radiation damage.[10,11] The increased susceptibility is due to larger sensitive volume and the low electric fields employed.* The operating bias voltage of the lithium drifted detectors is limited by the noise level of the detector since motion of lithium and thermal noise at high reverse bias creates a poor signal to noise ratio. The above factors will be correlated with radiation damage susceptibility in subsequent discussion.

Investigation of the radiation damage in lithium drifted detectors has been performed with electrons, gamma rays, neutron, proton, deuteron, and alpha particles.[10,11,12,13] In all cases the damage was evident by the increase in noise level, decrease in carrier lifetime and decrease in detector resolving power and collection efficiency. Extensive bombardment will render the detector inoperable.

The operation of a semiconductor detector is similar to the operation of an ionization chamber. Two collectors, the n- and p-sides of the junction, are separated by a depleted region of high resistivity. Incident radiation in the depleted region creates electron-hole pairs

---

*The reverse bias applied to lithium drifted detectors is typically a few hundred volts compared to a few thousand volts for non-lithium drifted detectors.

which are swept to the p- and n-side of the junction by an applied reverse bias. This rapid accumulation of charge produces the detector output signal. Radiation damage in the depleted region is produced when incident radiation creates vacancies and interstitials which in turn act as electron and hole traps. The traps reduce the carrier, electron or hole, lifetime. It is obvious when the trapping length for electrons and holes becomes less than the depletion width all of the charge is not collected and the detector has poor resolution. Lithium drifted detectors with larger depletion widths are consequently more susceptible to radiation damage.

The collection efficiency of a p-i-n junction detector can be expressed as follows:[10]

$$\eta = \frac{\mu\tau E}{w}\left[\, 1 - \exp(-w/\mu\tau E) \,\right] \qquad (1)$$

In the above expression μ represents the mobility of the carrier, τ is the carrier lifetime, E is the field strength in the depleted region, and w denotes the width of the depleted region. For a large collection efficiency, η, the trapping length, $\mu\tau E$, must be much larger than the depleted region width, w.

Methods to reduce the radiation damage have not been significantly successful. Scott found that masking the edges of the detector from incident radiation reduced its sensitivity to damage.[12] In addition, detectors kept under reverse bias were damaged less than detectors

exposed without bias. Mann irradiated lithium drifted detectors and found the threshold for deterioration of response to occur at 10^8 alphas/cm^2. He also demonstrated that the detectors could be redrifted and restored to their original condition even after exposure to 10^{12} alphas/cm^2.[13] Radiation defects in silicon are relatively stable at temperatures below 200°C.[15] Since Mann redrifted detectors between 135 and 150°C, thermal annealing of the defects is unlikely. The effective annealing must be due to a lithium-defect interaction.

It is essential to investigate the diffusion and mobility of lithium in silicon in order to comprehend the parameters involved in the selection of material for suitable solid state detectors. Furthermore, it is necessary to analyze lithium-defect interactions in order to evaluate the performance of lithium drifted detectors.

When lithium is introduced into silicon a shallow donor level 0.33 ev below the conduction band is created. Lithium ions are small (0.68 Å) and easily jump between interstitial sites as shown by its large diffusion coefficient. The mobility of lithium in silicon is critically dependent on the number and type of impurities. The analysis of lithium-acceptor interactions in silicon was performed by Reiss, et al,[16] who demonstrated that the lithium interacts electrostatically with the impurities, forming ion pairs that are immobile (contrasted with unpaired lithium) and hence reduce the effective diffusion coefficient of lithium in silicon.

Just as impurities in semiconductors drastically affect the mobility of lithium, defects also have a pronounced effect on the

movement of lithium in silicon. Initial studies on the interaction of impurities and dislocations in semiconductors employed copper ions in silicon and germanium.[17,18,19,20,21] Dash found that copper accumulated about dislocation lines and concluded that the copper precipitated at vacancy sites generated by such dislocations. This process will be discussed in Chapter II.

Resistivity studies on silicon and germanium saturated with lithium showed that the kinetics of lithium precipitation at vacancy sites followed an $\exp(\text{time})^{3/2}$ law.[22,23] The precipitation of lithium at radiation induced vacancies in silicon was first reported by Vavilov et al.[26,27] Upon electron and neutron irradiation of silicon saturated with lithium, Smirnova and Chapnin, with the use of Hall measurements, noted changes in the rate of production of various energy levels and attributed the lack of generation of acceptor energy levels in the range 0.05 to 0.23 ev above the valence band due to the precipitation of lithium.[14]

Diffusion in solids can take place via defects in the crystal.[24] Irradiation of silicon increases the number of defects which accelerate this diffusion process, but Lomer demonstrated that this increased mobility is a microscopic phenomena and not generally detectable with macroscopic diffusion measurements.[25]

The lithium diffusion coefficient has been measured in intrinsic and boron doped silicon with ion drift techniques[28,29] and it has been shown that the diffusion coefficient is reduced in doped silicon because immobile lithium-boron pairs are formed.

The quantitative effect of silicon defects on lithium mobility has not been determined to date. Attempts have been made to correlate the diffusion coefficient with dislocations introduced during crystal growth. However, this method was unsuccessful because the dislocations were not isotropically distributed.[29]

The purpose of this work is to determine the lithium diffusion coefficient in irradiated silicon and to study the lithium-vacancy interaction which reduces the lithium mobility. Irradiation of silicon with fast neutrons or high energy electrons produces isotropically distributed vacancies.

Lithium in irradiated silicon will either form pairs (P) with the vacancies, or precipitate (S) at the vacancy sites. Both of these interactions will reduce the lithium mobility in silicon.

With ion drift techniques, the mobility of lithium in silicon can be measured and the fraction of lithium ions paired (P/N) or the fraction precipitated (S/N) can be found from the ratio of the lithium mobility in irradiated silicon to the lithium mobility in intrinsic silicon (see Chapter II).

Lithium-vacancy pairs and lithium-vacancy precipitate have different equilibrium relations. Both of these relations can be expressed in terms of (P/N) or (S/N). It is possible to determine whether the lithium pairs or precipitates by evaluating the equilibrium expressions with measured values of (P/N) and (S/N). This is done in Chapter IV.

CHAPTER II

GENERAL THEORY

A. Ionization of Impurities in Semiconductors

This section describes the similarity between the action of impurities in semiconductors and the action of acids and bases in water. The expressions for ionization and equilibrium are presented along with the conditions necessary for this analogy to hold.

When lithium is introduced into silicon it ionizes in a way similar to the ionization of a weak base in water. Complete ionization occurs if the silicon is not saturated with lithium. The following ionization equations can be written for lithium and boron atoms in silicon:[4]

$$Li(Si) \rightleftharpoons Li^{+} + e^{-} \tag{1}$$

$$B(Si) \rightleftharpoons B^{-} + e^{+} \tag{2}$$

In the above equations Li(Si) represents atomic lithium in silicon, Li^{+} represents ionized lithium in silicon, and e^{-} denotes an electron liberated by the ionization. Similarly, B(Si), B^{-}, and e^{+} represent atomic boron, and ionized boron atom, and a hole liberated by the boron ionization.

Lithium in silicon is analogous to a base in water since it liberates an electron which corresponds to a hydroxyl ion, OH^-. Boron is analogous to an acid because it liberates a hole, e^+, which has properties similar to the hydronium ion, H^+. Appendix A gives a quantitative description of the semiconductor-water analogy.

For example, for weak acids and bases in water

$$NH_4OH \rightleftharpoons NH_4^+ + OH^- \tag{3}$$

$$HC_2H_3O_2 \rightleftharpoons C_2H_3O_2^- + H^+ \tag{4}$$

According to the law of mass action, the equilibrium relation for the ionization of ammonium hydroxide is[1]

$$\frac{[NH_4^+][OH^-]}{[NH_4OH]} = K \tag{5}$$

in which $[NH_4^+]$, $[OH^-]$, and $[NH_{4OH}]$, are the concentrations of the ammonium ion, the hydroxide ion, and the ammonium hydroxide, respectively. The equilibrium constant, K, is independent of the concentration of ammonium hydroxide and dependent only on temperature.

Similarly, the equilibrium relation for the ionization of lithium is silicon is

$$\frac{[Li^+][e^-]}{[Li(Si)]} = K_{Li} \tag{6}$$

The total concentration of lithium, N_{Li}, is equal to the concentration of the atomic lithium and the ionized lithium, i.e., $N_{Li} = Li^+ + Li(Si)$. With this relation equation (6) becomes,

$$\frac{[Li^+][e^-]}{[N_{Li}-Li^+]} = K_{Li} \tag{7}$$

If K_{Li} is a true equilibrium constant, it must be independent of the lithium concentration. This can be shown with the use of Fermi statistics. The concentration of atomic lithium, $[N_{Li} - Li^+]$, is actually the density of electrons in the donor level for a semiconductor material.

$$[N_{Li}-Li^+] = \frac{N_{Li}}{(1 + \frac{1}{2}\exp[(E_D-E_F)/kT])} \tag{8}$$

In equation (8), E_D is the energy of the lithium donor level, E_F is the Fermi level, k is the Boltzmann constant and T is the absolute temperature.

The total density of electrons in the conduction band is

$$[e^-] = \frac{\sum_j a_j}{(1 + \exp[(E_j-E_F)/kT])} \tag{9}$$

In the above equation a_j is the density of levels of energy E_j in the conduction band. It should be noted at this point that E_F, the Fermi level, depends on $[N_{Li} - Li^+]$ and $[e^-]$. The Fermi level is dependent on

the concentration of lithium in the semiconductor and cannot be present in the final expression for K_{Li}.

The unity in each of the Fermi density expressions can be considered small compared to the exponential terms if the assumption is made that E_D and E_j are much larger than E_F. Physically this means that the donors are almost completely ionized.

$$[N_{Li}\text{-}Li^+] = 2N_{Li} e^{E_F/kT} e^{-E_D/kT} \tag{10}$$

$$[e^-] = e^{E_F/kT} \sum_J a_j e^{-E_j/kT} \tag{11}$$

Rearranging equation (10), the expression for the concentration of ionized lithium atoms becomes

$$[Li^+] = N_{Li}[\, 1 - 2e^{E_F/kT} e^{-E_D/kT} \,] \tag{12}$$

Again neglecting the term $-2e^{E_F/kT} e^{-E_D/kT}$ because $(E_F - E_D)$ is large and negative, equation (12) reduces to

$$[Li^+] \cong N_{Li} \tag{13}$$

Finally, substituting equations (10), (11), and (13) into equation (7), the equilibrium expression for the ionization of lithium in silicon becomes

$$K_{Li} \cong \frac{\sum_J a_j e^{-E_j/kT}}{2 e^{-E_D/kT}} \tag{14}$$

The equilibrium constant, K_{Li}, does not contain E_F, hence is independent of the concentration of lithium. The quantities E_j, a_j, and E_D are constants also independent of concentration. The expression for K_{Li} given in equation (14) is valid under the condition that the ionization of the donors and acceptors is nearly complete.

The hole liberated by the ionization of a boron atom and the electron liberated by the ionization of a lithium atom also are in equilibrium.

$$e^+ + e^- \rightleftharpoons [e^+e^-] \tag{15}$$

This corresponds to the equilibrium of H^+ and OH^- in water.

$$H^+ + OH^- \rightleftharpoons [H^+OH^-] \tag{16}$$

Applying the law of mass action, equation (7), to the lithium ionization, the equilibrium

$$Li(Si) \rightleftharpoons Li^+ + e^-$$

will be driven to the right due to the removal of e^- by the formation of $[e^+e^-]$. For K_{Li} to remain constant, see equation (7), when $[e^-]$ is reduced, $[Li^+]$ must increase. Because the ionization of boron liberates e^+, the solubility of lithium in silicon will increase due to the presence of boron. Conversely, if phosphorus is present in the silicon instead of boron, the solubility of lithium will decrease because the ionization of phosphorus liberates an e^- driving the lithium ionization to the left.

$$P(Si) \rightleftharpoons P^{+} + e^{-} \tag{17}$$

In summary of the discussion regarding the ionization of impurities, consider all of the equilibrium reactions discussed in this section, equation (18), in terms of transitions on an energy level diagram, Figure 1.

$$\begin{aligned} Li(Si) &\overset{①}{\rightleftharpoons} Li^{+} + e^{-} \\ B(Si) &\overset{②}{\rightleftharpoons} B^{-} + e^{+} \\ & \qquad\qquad \uparrow\downarrow ③ \\ & \qquad\qquad e^{+}e^{-} \end{aligned} \tag{18}$$

As shown in Figure 1, transition ① between the lithium donor levels and the conduction band corresponds to the ionization of lithium. Transition ② corresponds to the ionization of boron and transition ③ represents hole-electron recombination and generation.

B. Ion Pairing

This section develops the relevant relations for lithium-boron pairing. The equilibrium constant, K_p, for an ion pair can be described in microscopic quantities, equation (41), or in macroscopic quantities, equation (23). Experimentally measured values of P/N can be used to

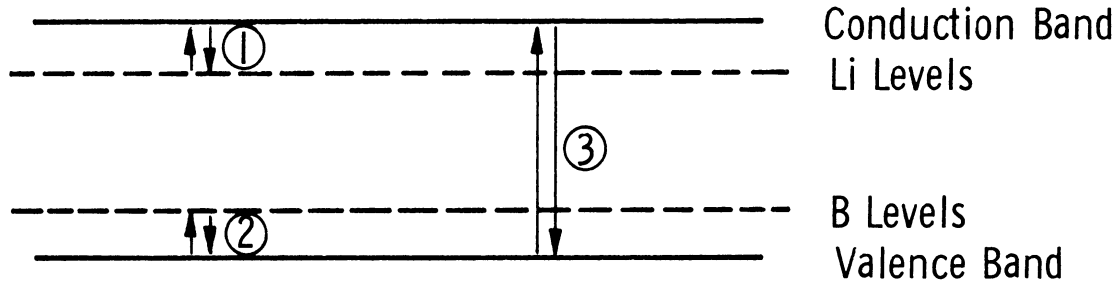

Fig. 1.--An energy band diagram for silicon showing the equilibrium relations ①, ② and ③.

find K_p with equation (23). After K_p is found, (a), the distance of closest approach of the ion pair can be calculated using equation (41).

The formation of an ion pair can be represented as follows:

$$\underset{\text{N, } \frac{\text{\# lithium ions}}{\text{cm}^3}}{Li^+} + \underset{\text{N, } \frac{\text{\# boron ions}}{\text{cm}^3}}{B^-} \rightleftharpoons \underset{\text{P, } \frac{\text{\# ion pairs}}{\text{cm}^3}}{[Li^+B^-]}$$

A mass action relation can be written for the above equilibrium by comparison to an electrolyte in water, see equation (5). If $[Li^+B^-]$ is represented by [P], then

$$\frac{[P]}{[Li^+][B^-]} = K_p \tag{20}$$

The total number of lithium ions, N, is equal to the number of paired plus the number of unpaired lithium ions. Similarly, the total number of boron ions, N, is equal to the number of paired plus the number of unpaired boron ions. Also assume that the total number of lithium ions is equal to the total number of boron ions.

$$N = Li^+ + P \quad ; \quad N = B^- + P \tag{21}$$

The quantities $[Li^+]$ and $[B^-]$ can be eliminated from equation (20) with equation (21).

$$\frac{[\,P\,]}{[\,N - P\,]^2} = K_p \tag{22}$$

$$\frac{[\,P/N\,]}{N[\,1 - P/N\,]^2} = K_p \tag{23}$$

Equation (23) describes the equilibrium constant, K_p, in terms of the fraction of ions paired, P/N.

Microscopic analysis of ion pairing was done by Bjerrum,[2] Fuoss,[3] and Reiss.[4] The work by Reiss is the most rigorous; however, the equations derived by the Bjerrum-Fuoss theory are easier to manage. The difference between the Reiss and Bjerrum-Fuoss analysis is minor except in the range of very high (>200°C) or very low (<0°C) temperatures. Since this set of experiments was conducted in the temperature range 30°C to 100°C, the Bjerrum-Fuoss theory will be applied.

At the equilibrium in a silicon medium containing equal concentrations of positive lithium and negative boron ions, each boron ion will have another ion as a nearest neighbor at a distance (r) away. Let $g(x)dx$ be the probability that a nearest neighbor lies in the shell $4\pi x^2dx$ about the boron ion. If the nearest neighbor is a lithium ion, the volume $4\pi r^3/3$, about the boron ion, must be devoid of ions, and the shell $4\pi r^2dr$ must be occupied by a lithium ion. Because $g(x)dx$ is the probability that a nearest neighbor lies in the shell $4\pi x^2dx$, the probability that a nearest neighbor does not lie in this shell is

$1 - g(x)dx$. The probability that the volume $4\pi r^3/3$ is empty is given by the following equation,

$$E(r) = 1 - \int_a^r g(x)dx \tag{24}$$

In the above equation, (a) is the distance of nearest approach of the two ions.

The probability that the shell $4\pi r^2dr$ is occupied by a lithium ion depends on the concentration of lithium ions at (r). This concentration will exceed the normal concentration, N, by an amount depending on (r), because of the coulomb attractive force between the lithium and the boron. If the concentration of the lithium ions at (r) is given by p(r), the probability in question becomes,

$$P(r) = 4\pi r^2 p(r)dr \tag{25}$$

Finally, the probability that the nearest neighbor is a lithium ion in the shell $4\pi r^2dr$ is a product of equations (24) and (25).

$$g(r) = E(r)P(r) \tag{26}$$

$$g(r) = \left[1 - \int_a^r g(x)dx \right] 4\pi r^2 p(r) \tag{27}$$

The solution to the above integral is obtained as follows:

Substitute $I = \int g(x)dx$ into equation (27).

$$\frac{dI}{dr} = (1 - I)4\pi r^2 p(r) \tag{28}$$

Rearrange the above equation and multiply by an integrating factor $e^{4\pi\int_a^r x^2 p(x)dx}$.

$$\frac{dI}{dr} e^{4\pi\int_a^r x^2 p(r)dx} + I4\pi r^2 p(r) e^{4\pi\int_a^r x^2 p(x)dx} = 4\pi r^2 p(r) e^{4\pi\int_a^r x^2 p(x)dx} \tag{29}$$

The following relation is obtained from equation (29) by combining the differential on the left side of the expression and integrating.

$$I\, e^{4\pi\int_a^r x^2 p(x)dx} = e^{4\pi\int_a^r x^2 p(x)dx} + C \tag{30}$$

The constant of integration, C, is evaluated at r = a, where I = 0. Consequently, (C) equals -1.

Multiply equation (30) by $e^{4\pi\int_a^r x^2 p(x)dx}$ and differentiate to obtain the following solution to equation (27)

$$\frac{dI}{dr} = g(r) = 4\pi r^2 p(r) e^{-4\pi\int_a^r x^2 p(x)dx} \tag{31}$$

The quantity p(r) must be determined to evaluate g(r). This can be accomplished by assuming coulomb interaction between a pair of nearest neighbors. Interaction between the next nearest neighbor is

ignored. The coulomb energy of the lithium-boron pair is

$$- q^2/\not{k}r \tag{32}$$

in which $\not{k}$ is the silicon dielectric constant and q is the charge of the lithium and boron ion. The concentration of the lithium ion, according to Boltzmann's law, at a distance (r) from the boron ion is

$$\begin{aligned} p(r) &= A \exp(q^2/\not{k}kTr) \\ k &= \text{Boltzmann's constant} \end{aligned} \tag{33}$$

The constant (A) in equation (33) is found to equal (N) by applying the boundary condition that p(r) must equal (N) at large (r). Equation (33) then can be written

$$p(r) = N \exp(q^2/\not{k}kTr) \tag{34}$$

The final expression for the probability that a lithium nearest neighbor is in the volume shell $4\pi r^2 dr$ about a boron ion is obtained by substituting equation (34) into equation (31).

$$g(r) = 4\pi r^2 N \exp[q^2/\not{k}kTr] \exp\left[-4\pi N \int_a^r x^2 \exp(q^2/\not{k}kTx)dx\right] \tag{35}$$

The function g(r) gives the fraction of lithium nearest neighbors that lie in the spherical shell of volume $4\pi r^2 dr$ about a boron ion. A plot of g(r) is shown in Figure 2, where (a) represents the

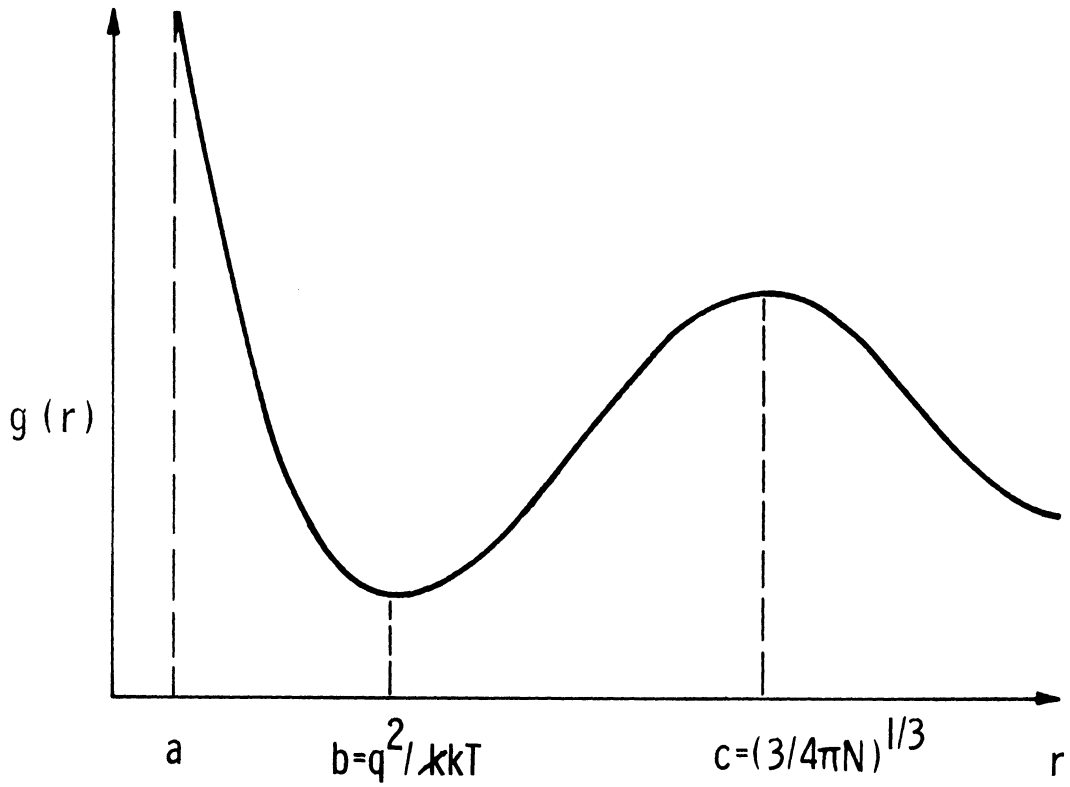

Fig. 2.--Equilibrium distribution of lithium nearest neighbors about a boron ion.

distance of closest approach between the lithium and the boron ion. Ion pairs are defined as all sets of neighbors separated by less than distance (b) apart.

To relate K_p to microscopic quantities, a dilute solution must be considered. In this case the number of lithium and boron ions, N, is small and the number of pairs, P, tends toward zero. Equation (22) becomes

$$\frac{P}{N^2} = K_p \tag{36}$$

or

$$\frac{P}{N} = NK_p \tag{37}$$

The fraction of paired ions, P/N, is also given by the expression;

$$\frac{P}{N} = \int_a^r g(r)dr \tag{38}$$

Substitution of equation (35) into equation (38) yields the following expression for the fraction of ions that are paired;

$$\frac{P}{N} = \int_a^r 4\pi r^2 N \exp(q^2/kTr)\exp\left[-4\pi N\int_a^r x^2\exp(q^2/kTx)dx\right] dr \tag{39}$$

For small (N) the exponential factor containing the integral in equation (39) can be replaced by unity.[4]

$$\frac{P}{N} = 4\pi N \int_a^r r^2 \exp(q^2/\epsilon kTr)\, dr \tag{40}$$

The equilibrium constant is obtained by combining equations (37) and (40).

$$K_p = 4\pi \int_a^r r^2 \exp(q^2/\epsilon kTr)\, dr \tag{41}$$

To calculate (a) it is necessary to know (K_p). The equilibrium constant can be found from P/N as shown in equation (23). The fraction ions paired, P/N, is found from the experimentally determined lithium mobility in the following manner: (The method by which lithium mobility is obtained from data is explained in section D.)

The overall mobility, μ, of the lithium ions in silicon is given by equation (42) if it is assumed that the paired ions represent neutral complexes that are immobile because the boron ions are substitutionally bound in the silicon crystal lattice.

$$\mu N = \mu_0 [Li^+] + \mu' [P] \tag{42}$$

or

$$\mu N = \mu_0 [N - P] + \mu' [P]$$

In the above equation, μ_o is the mobility of the unpaired lithium ions, and μ' is the mobility of the pairs, which is assumed to be zero. From equation (42)

$$\mu = \mu_o [\, 1 - P/N \,] \tag{43}$$

The fraction of paired lithium ions in boron doped silicon can be calculated from the ratio of the lithium mobility in boron doped silicon to the lithium mobility in intrinsic silicon.

$$P/N = 1 - \mu/\mu_o \tag{44}$$

At a constant temperature P/N can be calculated from a ratio of the lithium diffusion coefficients since $D = \frac{\mu kT}{e}$

$$P/N = 1 - D/D^o \tag{45}$$

To determine whether or not lithium pairs with an irradiation induced vacancy, $\frac{P/N}{(1 - P/N)^2}$ is plotted versus N (see equation 23), using values of P/N calculated from data obtained with irradiated samples. Since K_p is a constant, this plot must be linear if the lithium pairs with the vacancy. If the plot is not linear, the lithium does not pair with the vacancy. This calculation is performed in Chapter IV.

C. Lithium-Vacancy Precipitation

In this section, the relevant relations (equations 47 and 54) for lithium-vacancy precipitation are developed by comparison to an insoluble salt in water.

Lithium in silicon can be considered as a solution in which lithium ions are free to move from one interstitial site to another. An ion moving into a silicon vacancy, traps an electron, becomes atomic lithium and is immobile. This is similar to the precipitation of silver in a solution containing chlorine ions. The situations are not identical because the silicon vacancies are immobile so the lithium-vacancy precipitate, does not move but remains suspended in the crystal lattice.

In both cases the precipitate is in equilibrium with the ions,

$$Ag^{+} + Cl^{-} \rightleftharpoons AgCl \tag{46}$$

$$Li^{+} + D^{-} \rightleftharpoons S \tag{47}$$

In the above expression it is assumed that only one lithium precipitates at each vacancy site.[5]

The solubility product is an expression which describes the ion concentrations for partial ionization of AgCl.

$$[\,Ag^{+}\,][\,Cl^{-}\,] = K_{AgCl} \tag{48}$$

Equation (49) describes the lithium ion concentration in terms of a solubility product.

$$[\ Li^{+}\ ][\ D^{-}\ ] \quad = \quad K_S \tag{49}$$

Equations (48) and (49) describe saturated solutions.

Any alteration of the ion concentrations $[Li^{+}]$ or $[D^{-}]$, results in a spontaneous readjustment of the equilibrium by dissolution or precipitation so that the ion concentration product remains constant. The equilibrium constant K_s is a constant dependent only on temperature.

The quantity N_{Li} is defined as the total number of lithium atoms, both ionized and precipitated, and N_D is the total number of vacancies, both ionized and associated with lithium atoms.

$$N_L \quad = \quad Li^{+} \quad + \quad S \tag{50}$$

$$N_D \quad = \quad D^{-} \quad + \quad S \tag{51}$$

Substitution of equations (50) and (51) into equation (49) yields the result,

$$[N_L - S][N_D - S] \quad = \quad K_s \tag{52}$$

In a region where the number of lithium atoms and number of vacancies is equal, equation (52) can be reduced to

$$\begin{aligned} [\, N - S \,]^2 &= K_s \\ N &= N_{Li} = N_D \end{aligned} \tag{53}$$

Rearrangement of equation (53) results in the following expression:

$$N[\, 1 - S/N] = K_s^{\frac{1}{2}} = K_s' \tag{54}$$

To evaluate this model, S/N, the fraction of lithium precipitated, must be determined. This is accomplished in the same manner as discussed previously (see equations 44 and 45). If the precipitate is assumed immobile, the overall mobility of the lithium in silicon with radiation induced vacancies will be

$$\mu = \mu_0 [\, 1 - S/N \,] \tag{55}$$

The fraction of lithium atoms precipitated is calculated from the ratio of mobility of lithium in irradiated silicon, μ , to the mobility of the lithium in unirradiated silicon, μ_0 .

$$S/N = 1 - \mu/\mu_0 \tag{56}$$

In terms of diffusion coefficients

$$S/N = 1 - D/D^0 \tag{57}$$

To determine whether or not lithium precipitates at a vacancy site, (1 - S/N) is plotted versus 1/N (see equation 54) using values of S/N calculated from data obtained with irradiated samples. Since K_s' is a constant, this plot must be linear if the lithium precipitates at the vacancy sites. If the plot is not linear, the lithium does not precipitate at the vacancy sites. This calculation is performed in Chapter IV.

D. Determination of Lithium Ion Mobility

The lithium mobility in silicon must be known in order to calculate P/N, K_p, a, S/N, and K_s'. This section describes the method used to find the mobility. An expression is derived, equation (83), by which the mobility can be calculated from the measured capacitance of a silicon diode. The diode capacitance is plotted as $(10^3/C)^2$ versus drift time and the derivative of this curve provides the predominate factor in equation (83).

The ionic mobility of lithium can be determined from the drift (motion) of lithium ions in an electric field. The electric field in a p-n junction under reverse bias is high and it might be surmised that the motion of lithium ions would be observable if it were present in a p-n junction. If a diode is prepared using boron as the acceptor (p-side) and lithium as the donor (n-side), the junction region is an area where the number of lithium ions is equal to the number of boron ions.[6]

A diode can be formed by diffusing lithium into boron doped silicon. (Details of the method of diode construction and crystal preparation will be discussed in Chapter III.) The dependence of the

lithium concentration, N_{Li}, on space and time within the crystal is expressed by the diffusion equation;

$$\frac{\partial N_{Li}}{\partial t} = D\nabla^2 N_{Li} \tag{58}$$

D = diffusion coefficient

Equation (59) is a solution to equation (58) for the following conditions:[7]

1. The lithium concentration at the surface of the crystal remains constant throughout the diffusion period, and equal to N_o.
2. The crystal is instantly heated to a temperature T, for a period of time t_o.
3. At time t_o the crystal is instantly cooled to ambient temperature.
4. The diffusion coefficient at temperature T is D_o.
5. The crystal is considered a semi-infinite solid.
6. The distance (x) is measured from the surface of the crystal inward.

$$N_{Li} = N_o \operatorname{erfc}\left[x/2(D_o t_o)^{\frac{1}{2}}\right] \tag{59}$$

Figure 3 is a plot of equation (59) and illustrates the lithium distribution after the initial diffusion.

When a reverse bias is placed across the diode (at a drift temperature much lower than the initial diffusion temperature), the

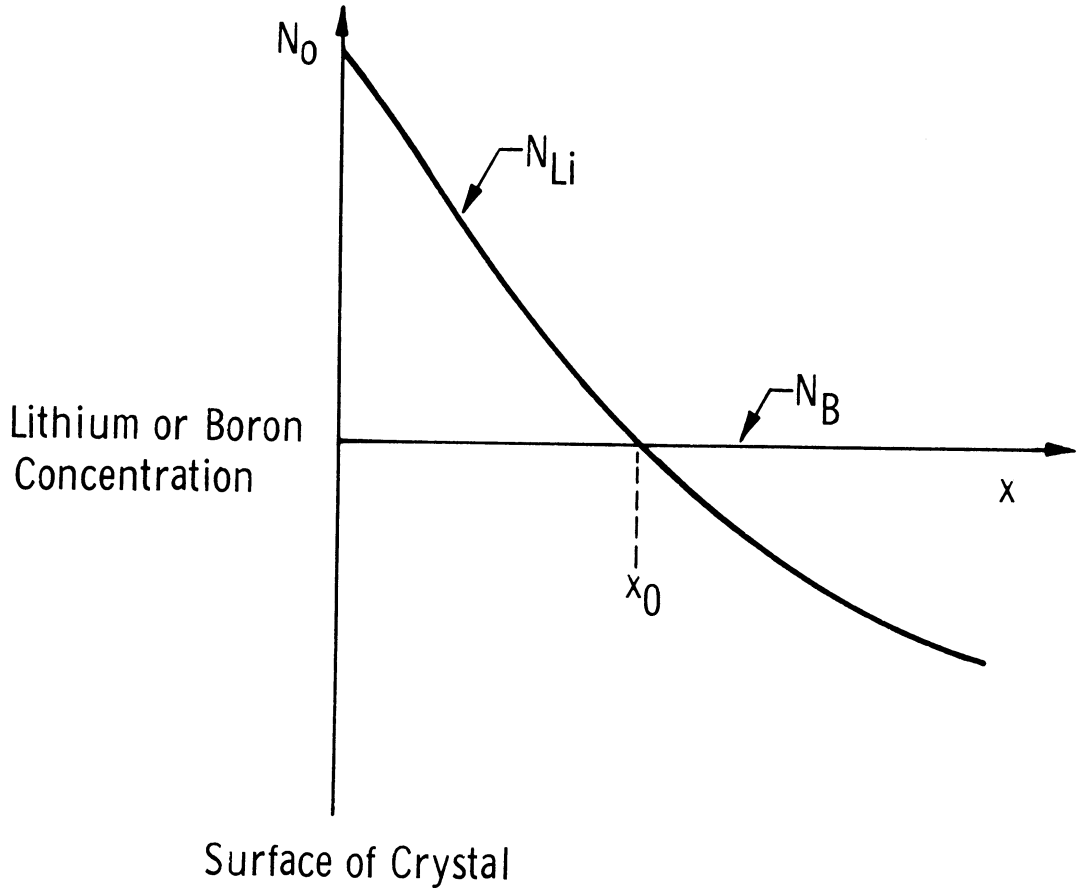

Fig. 3.--Lithium distribution (N_{Li}) in silicon after an initial diffusion period t_o. The quantity N_B represents the boron concentration in the silicon.

electrostatic field present in the space charge region near (x_o) will exert a force tending to move the positively charged lithium ions from the n-side of the junction to the p-side.

In the junction area the motion of lithium due to diffusion is negligible compared to the motion of the lithium due to the electrostatic field:[8]

$$E\mu N_{Li} \gg D\nabla N_{Li} \tag{60}$$

The large electrostatic field exists only in the region where N_{Li} is approximately equal to N_B and the number of lithium ions per cm^2 drifted across the junction in time t, is expressed by

$$E\mu N_{Li}\, t = E\mu N_B\, t \tag{61}$$

As lithium drifts across the junction its concentration to the left of (x_o) will decrease and its concentration to the right of (x_o) will increase. In this process the lithium will form ion pairs with the substitutionally bound boron. It is imperative to observe that N_{Li} to the left of (x_o) cannot decrease below N_B. This is illustrated in Figure 4. Excess boron ions to the left of (x_o) would alter the space charge causing the lithium ions to move into it until the number of lithium ions equaled the number of boron ions. For the same reason it can be ascertained that the lithium ion concentration cannot rise above N_B to the right of (x_o).

The gradient of the lithium concentration at (x_1) and (x_2) in Figure 4 can be approximated by straight vertical lines because of the

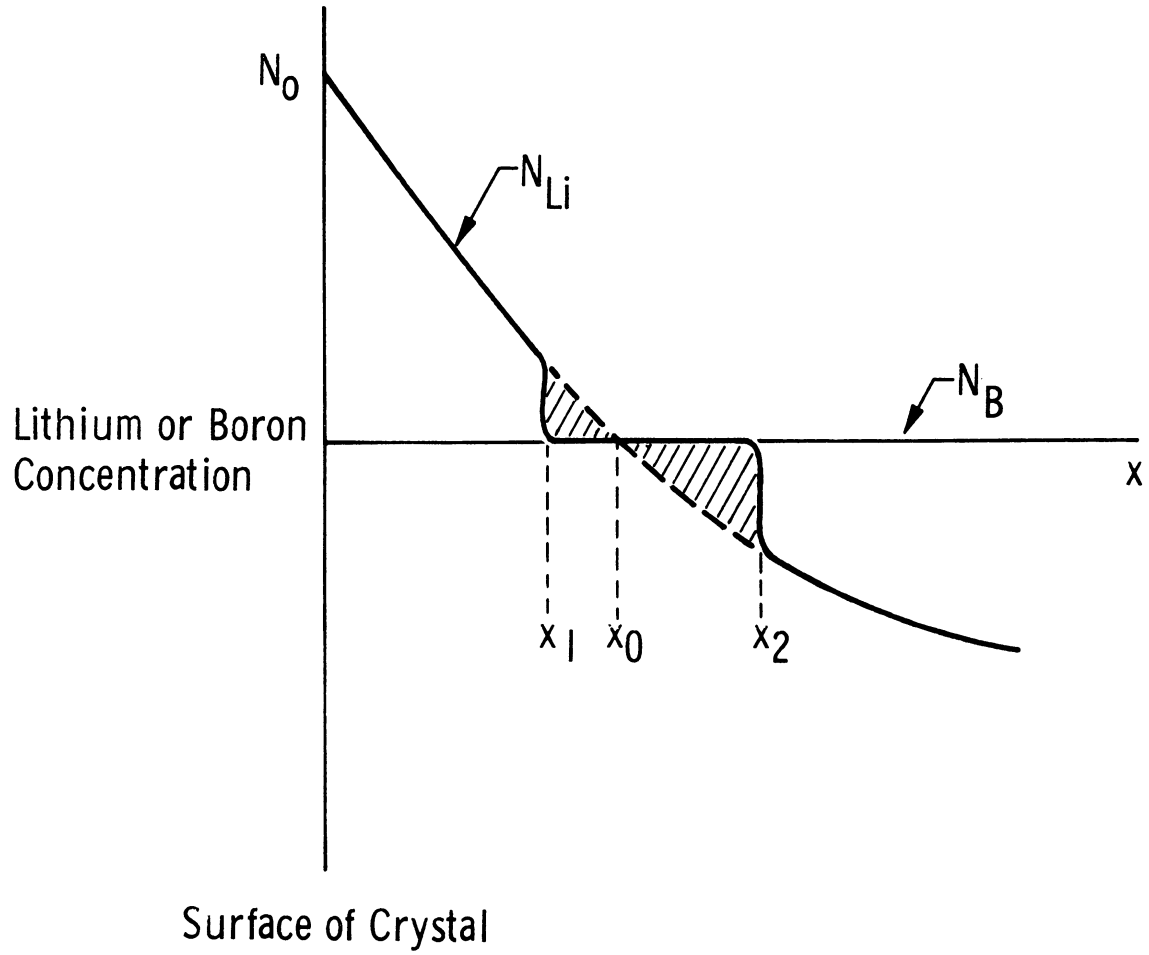

Fig. 4.--Lithium distribution (N_{Li}) in silicon after a period of ion drifting, t.

large field present between these two points. The concentration gradient in the zero field region at (x_1) supplies the lithium ions by diffusion to the drift region

$$D\nabla N_{Li} = E\mu N_{Li} \tag{62}$$

The amount of lithium drifted in time (t) is represented by the cross-hatched area in Figure 4 and the following expressions

$$\int_0^t E\mu N_B dT = \int_{x_1}^{x_o} N_{Li}\, dx - [x_o - x_1]N_B \tag{63}$$

$$\int_0^t E\mu N_B dt = [x_2 - x_o]N_B - \int_{x_o}^{x_2} N_{Li} dx \tag{64}$$

Equation (65) is obtained by substituting equation (59) into equation (63).

$$\int_0^t E\mu N_B\, dt = \int_{x_1}^{x_o} N_o\, \mathrm{erfc}[x/2(D_o t_o)^{\frac{1}{2}}]\, dx - (x_o - x_1)N_B \tag{65}$$

The integral on the right hand side of equation (65) can be integrated by parts. The equation for the amount of lithium drifted in time (t) following this integration is

$$\int_0^t E\mu N_B dt = x_o N_o \operatorname{erfc}[x_o/2(D_o t_o)^{\frac{1}{2}}] - x_1 N_o \operatorname{erfc}[x_1/2(D_o t_o)^{\frac{1}{2}}] + \frac{2N_o}{\sqrt{\pi}}(D_o t_o)^{\frac{1}{2}}[\exp(-x_1^2/4D_o t_o) - \exp(-x_o^2/4D_o t_o)] - (x_o - x_1) N_B \quad (66)$$

For long drift time the co-error function term in equation (66) can be expanded as follows:[8]

$$\operatorname{erfc} x = \frac{e^{-x^2}}{x\sqrt{\pi}} - \frac{e^{-x^2}}{2x^3\sqrt{\pi}} \cdots\cdots\cdots\cdots\cdots \quad (67)$$

This expansion reduces equation (66) to equation (68).

$$\int_0^t E\mu N_B \, dt = \frac{4N_o(D_o t_o)^{3/2}}{x_o^2\sqrt{\pi}} \left(\frac{x_o^2}{x_1^2} \exp[(x_o^2 - x_1^2)/4D_o t_o] - 1 \right) X \exp[-x_o^2/4D_o t_o] - (x_o - x_1) N_B \quad (68)$$

To reduce equation (68) it is necessary to evaluate N_B in terms of (x_o). This can be accomplished by expanding equation (59) with equation (67) and applying the boundary condition at $x = x_o$, $N_{Li} = N_B$.

$$N_{Li} \cong [2N_o(D_o t_o)^{\frac{1}{2}}/x\sqrt{\pi}] \exp(-x^2/4D_o t_o) \quad (69)$$

$$N_B \cong [2N_o(D_o t_o)^{\frac{1}{2}}/x_o\sqrt{\pi}] \exp(-x_o^2/4D_o t_o) \quad (70)$$

Substitution of expression (70) into (68) yields

$$\int_0^t E\mu N_B dt = \frac{2N_B(D_o t_o)}{x_o}\left(\frac{x_o^2}{x_1^2} \exp[(x_o^2 - x_1^2)/4D_o t_o] - 1 \right) - (x_o - x_1)N_B \tag{71}$$

If (Z) is defined as $2D_o t_o/x_o$, the equation for the amount of lithium drifted in time (t) becomes

$$\int_0^t E\mu dt = Z\left(\frac{x_o^2}{x_1^2} \exp[(x_o^2 - x_1^2)/4D_o t_o] - 1 \right) + x_1 - x_o \tag{72}$$

A similar expression can be derived for the amount of lithium drifted in time (t) utilizing the right half of the junction.

$$\int_0^t E\mu dt = -Z\left(1 - \frac{x_o^2}{x_2^2} \exp[(x_o^2 - x_2^2)/4D_o t_o] \right) + x_2 - x_o \tag{73}$$

The desired expression for the mobility of lithium in terms of junction capacitance can be derived from equations (72) and (73). For long drift time (t), (several hours), $(x_2^2 - x_o^2) \gg 4D_o t_o$.[8] With this condition equation (73) reduces to

$$\int_0^t E\mu dt = x_2 - x_o - Z \tag{74}$$

If (V) is the reverse voltage applied across the junction and (W) is the width of the junction the electrostatic field in the junction is given by V/W.

$$\int_0^t \left(\frac{V}{W}\right)\mu dt = x_2 - x_o - Z \tag{75}$$

The following equation arises from equating equation (74) to equation (72).

$$Z\left[(x_o/x_1)^2 \exp[(x_o^2 - x_1^2)/4D_o t_o] - 1\right] + x_1 - x_o = x_2 - x_o - Z \tag{76}$$

The junction width (W) is equal to $(x_2 - x_1)$ so equation (76) becomes

$$Z\left[(x_o/x_1)^2 \exp[(x_o^2 - x_1^2)/4D_o t_o]\right] = W \tag{77}$$

For long drift time the junction primarily expands to the right, consequently $x_o = x_1$.[8] Taking the logarithm of equation (77) and employing this approximation

$$\text{Ln } (W/Z) = \frac{x_o + x_1}{4D_o t_o}(x_o - x_1) \tag{78}$$

Under the consideration that $(x_o + x_1)/4D_o t_o$ is approximately $2x_o/4D_o t_o$ and that $Z = 2D_o t_o/x_o$, equation (78) becomes

$$x_o - x_1 = Z \text{ Ln } (W/Z) \tag{79}$$

Equation (79) and (75) can be combined to eliminate the quantity x_o.

$$\int_0^t \left(\frac{V}{W}\right)\mu \, dt = W - Z - Z \text{ Ln } (W/Z) \tag{80}$$

Differentiation of equation (80) with respect to time and subsequent rearrangement yields an expression for the lithium mobility in terms of the junction width and reverse bias.

$$\mu = \left(\frac{1 - Z/W}{V}\right) W \frac{dW}{dt} \tag{81}$$

or

$$\mu = \left(\frac{1 - Z/W}{2V}\right) \frac{dW^2}{dt}$$

The capacitance of a junction is inversely proportional to the junction width as shown below

$$C = k\epsilon_o \frac{A}{W} \tag{82}$$

$k\epsilon_o$ = the permittivity of silicon

A = area of junction

Insertion of equation (82) into (81) yields an expression for lithium mobility in terms of junction capacitance.

$$\mu = \frac{X(X - Z/W_A)}{2V} \frac{d}{dt}(10^3/C)^2 \tag{83}$$

In the above equation (C) is the junction capacitance measured in pico-farads, (Z) is equal to $2D_o t_o/x_o$ as previously defined, and (V) is the applied reverse bias measured in volts. The quantity (X) is proportional to the junction area as shown below.

$$X = (k \epsilon_o A) \times 10^3 \tag{84}$$

Finally, (W_A) represents the average width of the junction during the time the slope $\frac{d}{dt}(10^3/C)^2$ was measured and is expressed in units of $(10^3/C)$.

In order to find the lithium mobility, the junction capacitance $(10^3/C)^2$ must be plotted versus the drift time, (t), and the slope of this curve measured, $\frac{d}{dt}(10^3/C)^2$.

This concludes the theory section. Further elucidation of some quantities discussed can be found in Appendix B, sample calculations. In particular, this applies to the quantities introduced in equation (83).

CHAPTER III

EXPERIMENTAL PROCEDURE

A. Diode Preparation

This study required the use of silicon as free from defects as possible. Previous studies indicated that lithium could not be drifted in silicon having a dislocation density greater than 30,000/cm^2.[1] The silicon selected for this study had a boron concentration of 1.6 x 10^{14} atoms/cm^3 (100 ohm-cm) and an oxygen concentration below 5 x 10^{12} atoms/cm^3.

To prepare a diffused junction, a silicon wafer (20 mm diameter x 2 mm thick) was first lapped to remove scratches, then ultrasonically cleansed and finally degreased in carbon tetrachloride. Lithium-in-oil suspension was subsequently brushed onto the lapped surface and dried at 150°C in a diffusion furnace. (See Figure 5.) The wafer was pushed into the center of the furnace (420°C) after the drying period, and the lithium diffused into the crystal. The wafer was then quickly removed from the furnace and dropped into a beaker of methyl alcohol for quenching.

The surface was again lapped to remove pits caused by lithium diffusion. The uniformity of penetration was evaluated by measuring the surface resistance with a two point probe. Diodes with resistance greater than 200 ohms on the n-side were discarded.

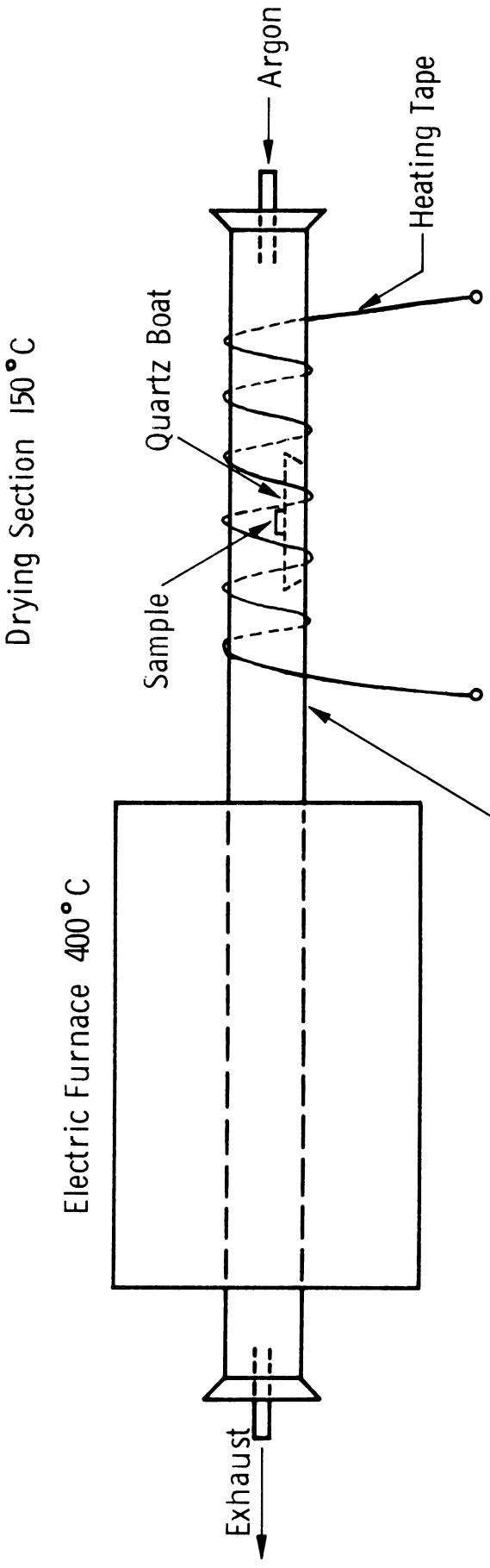

Fig. 5.--A tube diffusion furnace.

The two point probe measurements indicated that the lithium was not distributed uniformly to the edge of the wafer. For this reason the edge portion of the diode was removed by dicing the crystal into four small samples which measured 0.25 inches square. (See Figure 6.)

Nickel contacts were applied to the diodes by electroless plating[2] after the dicing operation. Next, a solution of Apiezon W wax in trichlorethylene was painted on the two sides of the sample and allowed to dry. The nickel on the edges of the diode was removed with a mixture of HNO_3 and HF and then the protective Apiezon wax was removed, completing the diode preparation (see Figure 7).

The small junctions were tested individually with a reverse bias of 100 volts. Diodes with less than 50 microamperes reverse current were used in this experiment.

B. Neutron Irradiation

Samples were neutron irradiated in an empty core position of the Ford Nuclear Reactor for periods of five to thirty minutes at two megawatts reactor power level. The epithermal flux was 2×10^{11} neutrons/cm^2sec and the cadmium ratio was 10.

The diodes were wrapped in rubber diaphrams and placed in polyethylene bottles that were ballasted with bismuth metal. Neither the silicon nor the nickel contacts were noticeably activated because of the short exposure duration and small absorption cross sections of silicon (0.12 barns) and of nickel (4.6 barns).

To isolate effects produced by thermal neutrons from effects produced by fast neutrons, identical samples were irradiated with and

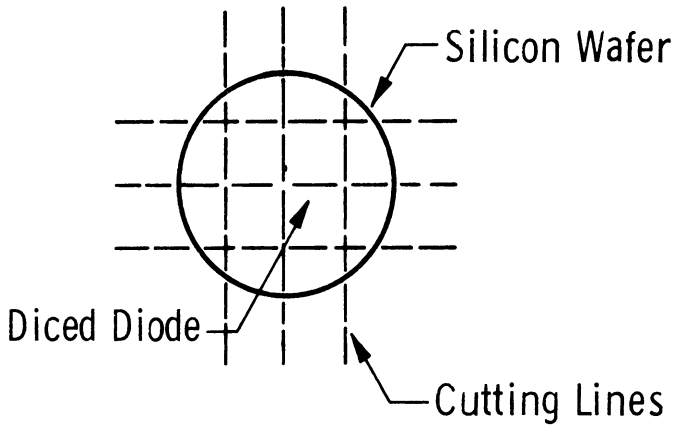

Fig. 6.--Dicing the wafer diode.

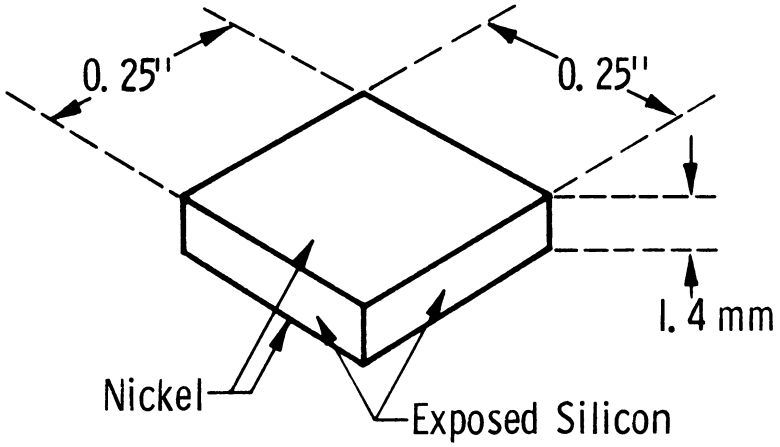

Fig. 7.--A prepared lithium diffused diode.

without a 0.040 inch cadmium cover. The difference between changes produced by reactor irradiation without a cadmium cover and with the cadmium protector was interpreted to be the effects produced by thermal neutrons.

Gold foil technique was used to determine the neutron flux in the reactor. Two gold foils (approximately 1/8 inch square by 0.001 inch thick) were included in each sample bottle, one with a cadmium cover and the other bare. Activation of the gold was measured with a 3 x 3 inch NaI:Tl well counter. The rate of production of Au^{198}, R, for the bare and cadmium covered foils is[3]

$$R = \frac{C/f}{(1 - e^{-\lambda t_1}) e^{-\lambda t_2}} \qquad (1)$$

In the above expression, (C) represents the specific activity of the gold, corrected for background, and (f) is the efficiency of the well counter (52.2%). In the exponential terms, (t_1) is the reactor exposure time, and (t_2) denotes the time interval between removal of the sample from the reactor to the measuring of the gold activity. Finally (λ) expresses the decay constant for gold (1.07×10^{12} hr^{-1}).

From equation (1), the thermal, Φ_{th}, and fast, Φ_{epi} fluxes of the reactor can be calculated.

$$\Phi_{th} = \frac{(R_b - R_c)}{\epsilon N_D \langle \sigma a \rangle th} \qquad (2)$$

$$\Phi_{epi} = \frac{R_c}{\epsilon N_D \langle \sigma a \rangle epi} \qquad (3)$$

In equations (2) and (3), R_b represents the rate of production of Au^{198} in the bare gold foil and R_c denotes the rate of production of Au^{198} in the cadmium covered foil. The quantity (ϵ) is a flux depression correction factor, (ϵ = 1.0 for silicon) and N_D gives the number of nuclei in the gold foil. The average microscopic cross section over the thermal portion of the reactor neutron spectrum is given by $\langle \sigma_a \rangle_{th}$. Similarly, the effective microscopic cross section for neutrons with energy greater than 0.4 ev (the cadmium cutoff) can be expressed as;

$$\langle \sigma_a \rangle_{epi} = \int_{E=0.4 \text{ ev}}^{\infty} \frac{\sigma_a(E)}{E} dE \qquad (4)$$

C. Electron Irradiation

Electron bombardment was performed at Wright-Patterson Air Force Base in Dayton, Ohio, with a one MeV Van de Graaf generator. Relatively high energy electrons (0.9 MeV) were used so that the flux directed into the diode samples would not vary excessively over a penetration depth of about 0.1 mm. The range of the 0.9 MeV electrons is approximately 1.4 mm in silicon. A dose correction factor was calculated and presented in Chapter IV. Figure 8 outlines the bombardment technique.

The size of the electron beam was adjusted electrostatically to the approximate area of the sample. By employing a Faraday cup, the electron flux was fixed at 1 x 10^{17} electrons/(area of diode)-hr so that exposure times ranged from three to twenty minutes. The sample

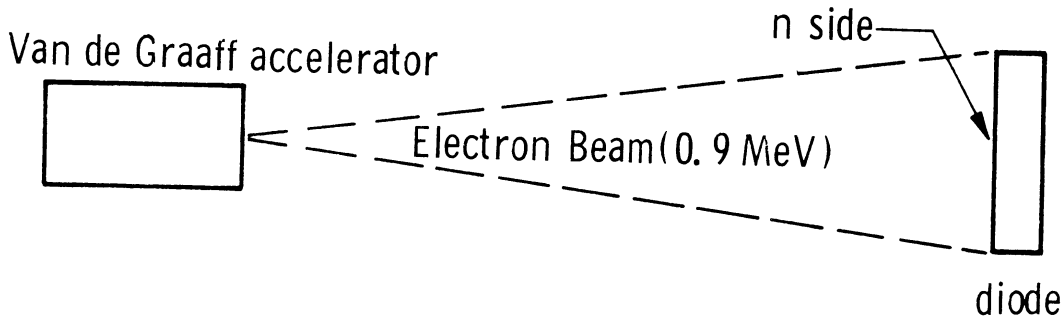

Fig. 8.--Electron bombardment of the diced diode.

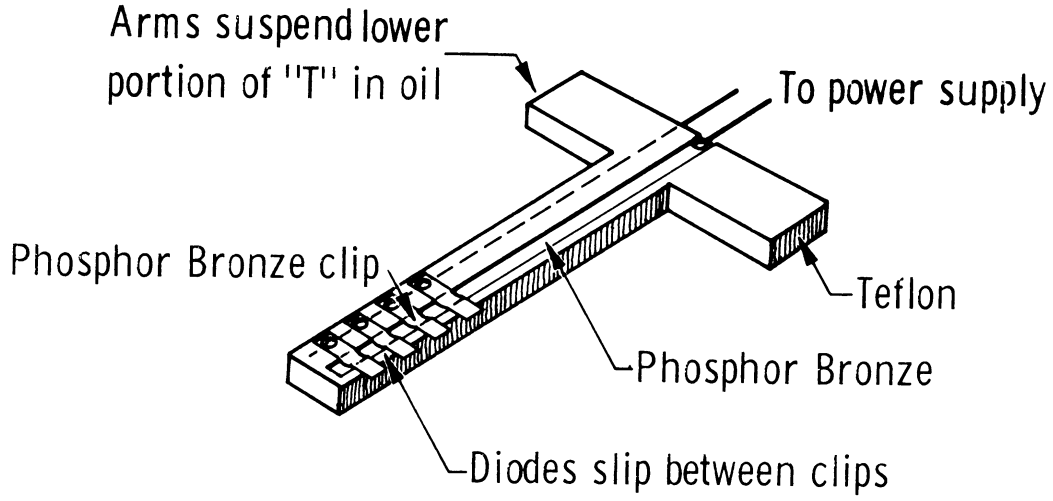

Fig. 9.--Jig designed to hold several diodes in a constant temperature bath.

temperature rise was limited to less than 10°C (above room temperature) by passing compressed air over the diode during irradiation.

Because of the finite range of the electrons in silicon, the diodes were bombarded on the n-side and without nickel contacts, as is illustrated in Figure 8. Following the electron bombardment, nickel contacts were applied as outlined previously.

D. Gamma Irradiation

Gamma irradiation was performed with the Phoenix Project 10,000 curie Co^{60} source. The irradiation was straightforward with the diodes placed in the center of Co^{60} rod assembly. The dose rate was 925 kilorads per hour and exposure periods ranged from ten to several hundred hours.

E. Lithium Drift and Diode Capacitance Measurement

The field present in a reverse biased diode is sufficient to move the lithium ions as described in Chapter II. The movement of the ions and the formation of lithium-vacancy precipitate cause the junction capacitance to decrease. Measurement of the junction capacitance with respect to time provides a method to investigate the precipitation process in irradiated silicon. The data is obtained in the following manner:

To drift the lithium in the junctions, several were held in a constant temperature bath of transformer oil under reverse bias with a jig constructed of teflon and phosphor bronze (see Figure 9). The

transformer oil provided a medium for good heat transfer yet high electrical resistivity. Parallel circuitry allowed a reverse bias to be applied to many diodes with a single D. C. power supply.

The diode capacitance was measured one at a time outside the bath using a Tektronix direct reading bridge and a 90 volt battery to supply the bias. The internal capacitance of the battery was blocked from the bridge so that it did not mask the junction capacitance. A 0.5 henry choke in series with the battery stopped all but 5% of the bridge signal making it possible to balance it with the battery connected. The bridge was recalibrated from time to time with precision capacitors in the range of 5 pf to 500 pf.

The capacitance of each junction was measured and recorded chronologically for periods up to 1000 hours. Analysis of these results is presented in the following chapter.

CHAPTER IV

ANALYSIS AND DISCUSSION OF RESULTS

A. Determination of Lithium Mobility in Boron Doped Silicon

It was requisite to determine the mobility of lithium in boron doped silicon not only to select material in which lithium boron pairing would not interfere with the lithium-vacancy precipitate, but to insure that the results of measurement and analysis compared favorably with previously reported values of lithium mobility. With this in mind, the following results on boron doped silicon are presented.

A typical plot of $(10^3/C)^2$ versus drift time is given in Figure 11 (the control sample) for 100 ohm-cm boron doped silicon drifted at 30°C with a reverse bias of 100 volts. The value of the slope of the curved inserted in equation (83) gives $\mu = 8.2 \times 10^{-12}$ cm^2/volt-sec for the mobility of lithium in the sample. The diffusion coefficient obtained from the Einstein relation

$$D = \frac{\mu kT}{e} \tag{1}$$

is $D = 2.5 \times 10^{-13}$ cm^2/sec. The sample, in which the number of boron atoms was 1.6×10^{14} atoms/cm^3, did not reduce the lithium diffusion

coefficient beyond its range of values in intrinsic silicon for temperatures above 30°C.[1,2] This is shown in Figure 10 with the lithium diffusion coefficient for silicon containing larger amounts of boron.[3] Consequently, lithium-boron pairing will be considered negligible compared to lithium-vacancy precipitate in reducing the diffusion coefficient.

The curves for the diffusion coefficient shown in Figure 10 confirm the theory of ion pairing developed in Chapter II. From the ratio of the diffusion coefficient in boron doped silicon to the diffusion coefficient in intrinsic silicon at the same temperature, the fraction, P/N, can be calculated.

$$P/N = 1 - \mu/\mu_o \tag{2}$$

or

$$P/N = 1 - D/D^o \tag{3}$$

After calculating P/N from equation (3), the equilibrium constant for ion pairing, K_p, can be found from the quotient,

$$K_p = \frac{P/N}{N[1 - P/N]^2} \tag{4}$$

Finally, utilizing equation (II-41), the distance of closest approach, (a), can be calculated for the lithium boron pair. Results of this

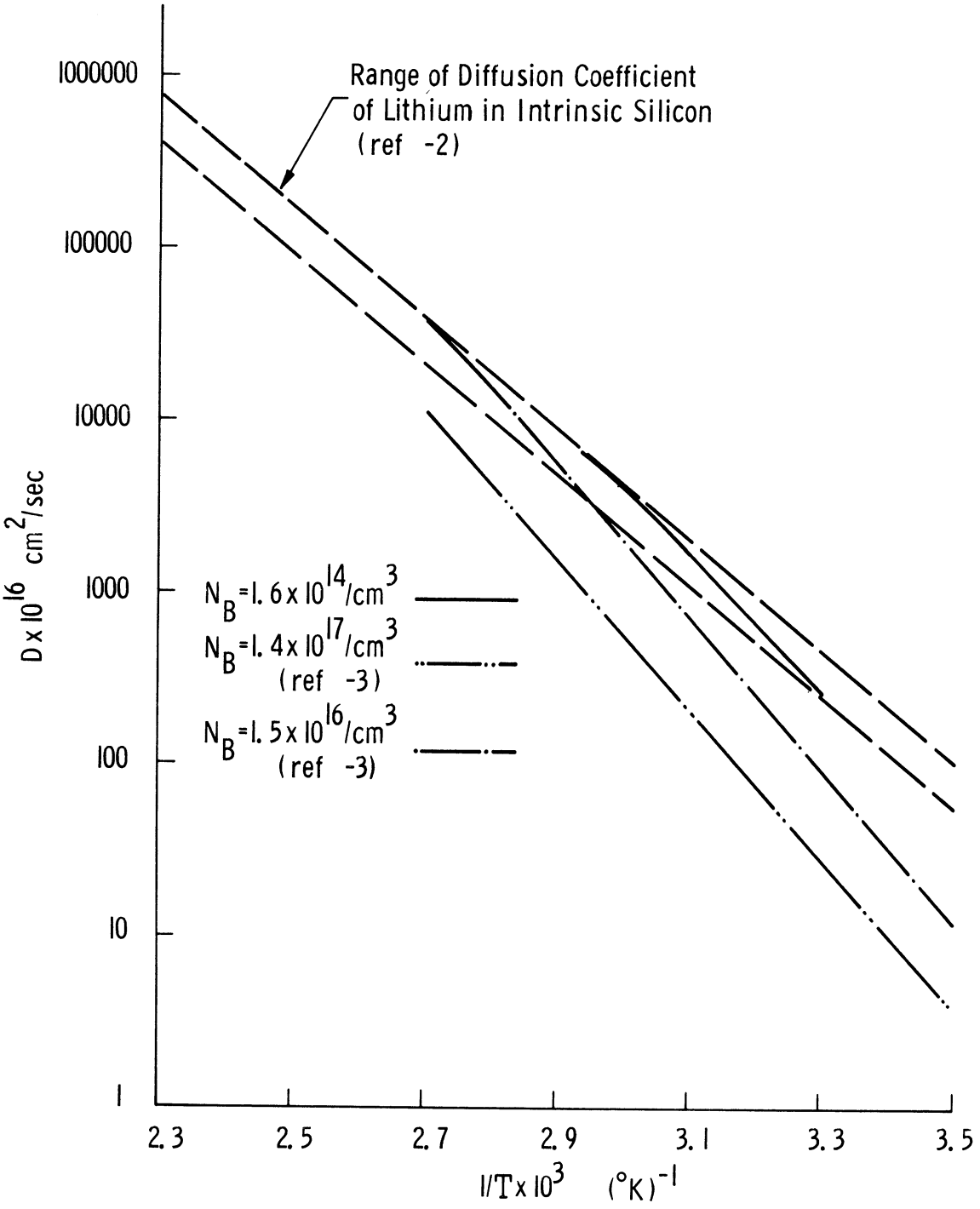

Fig. 10.--Effect of boron concentration on lithium diffusion coefficient in silicon.

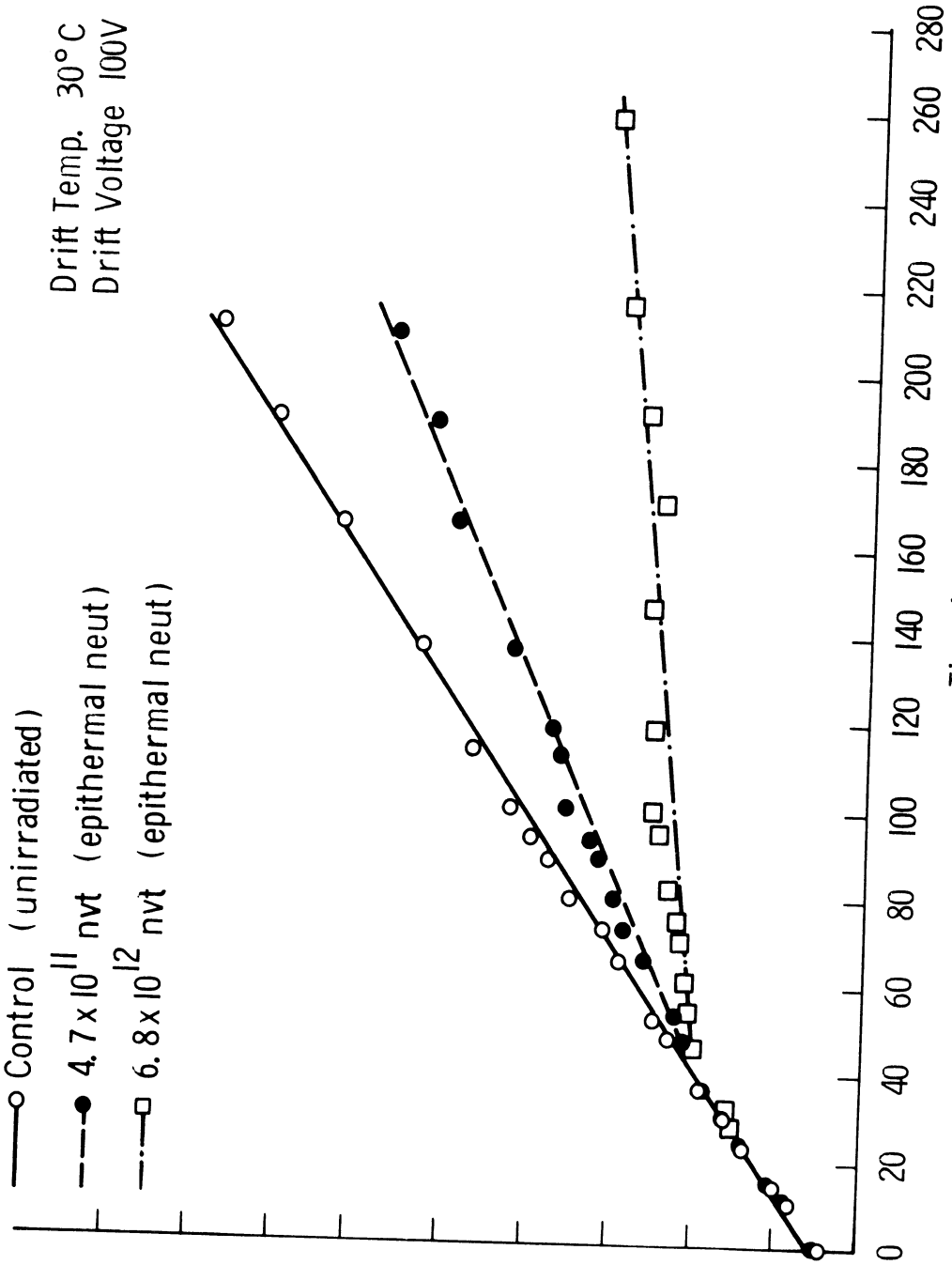

Fig. 11.--$(10^3/C)^2$ versus drift time for neutron irradiated silicon diodes.

calculation show that (a) ranges from 2.5 to 2.7 Å. Calculated values of K_p using equation (II-41) with a = 2.5 Å compare favorably to values calculated with equation (4) for all temperatures between 30°C and 150°C.[3]

B. Lithium Mobility in Neutron Irradiated Silicon

Following neutron irradiation the samples were drifted at various temperatures. In general, three of the four diodes cut from a single wafer were irradiated while the fourth was kept for control. The results of all drift measurements were discarded if the lithium diffusion coefficient calculated from the control sample data did not fall within the range of values for intrinsic silicon shown in Figure 10.

Figure 11 illustrates a representative plot of $(10^3/C)^2$ versus drift time for neutron irradiated diodes. The initial rapid rise of the curve is typical and represents an effect caused by vacancies formed in the immediate junction area. The lithium in the junction tends to move during irradiation because of the built-in-field present. As it moves, the lithium will precipitate at vacancy sites and produce an intrinsic area in and near the junction. Hence, the initial drift rate of the lithium in the irradiated silicon will be identical to its drift rate in unirradiated intrinsic silicon.

As the junction widens during the drifting period, the lithium advances into the p-side of the junction, hence the slope of the curves shown in Figure 11 decreases and remains constant at a lower value than the unirradiated sample. In this region the lithium-vacancy precipitate

reduces the effective mobility of lithium, and the quantity $\frac{d}{dt}(10^3/C)^2$ is measured to be used in the determination of the lithium diffusion coefficient.

To substantiate that the mobility of lithium is being reduced by lithium-vacancy precipitation in the p material rather than some phenomena caused by an irradiated junction, the following annealing study was performed.

Three junctions were bombarded with 2.2×10^{14} epithermal neutrons/cm^2. Two of the samples were heated to 400°C for five minutes and ten minutes, respectively. Afterwards, the three junctions were drifted at 100°C under reverse bias (50 volts) simultaneously with an unirradiated junction. Upon termination of drifting, which was continued for more than ten hours, the previously unheated irradiated junction was heated to 400°C for five minutes and then redrifted at 100°C with 50 volts reverse bias. The results are shown in Figure 12. Some annealing of the vacancy defects was observed because the slopes of curves C and B are greater than the slope of curve A; however, the slopes of these curves are far less than the unirradiated sample.

Heating of the irradiated diodes diffuses the lithium deeper into the crystal creating a new junction. Because the mobility is reduced in irradiated samples with junctions created after irradiation, the reduction must be due to lithium-vacancy precipitation.

The relative effects of fast and slow neutrons on the lithium drift rate is shown in Figure 13. Samples A and B were irradiated with and without a cadmium wrap. No measurable difference in the slopes of

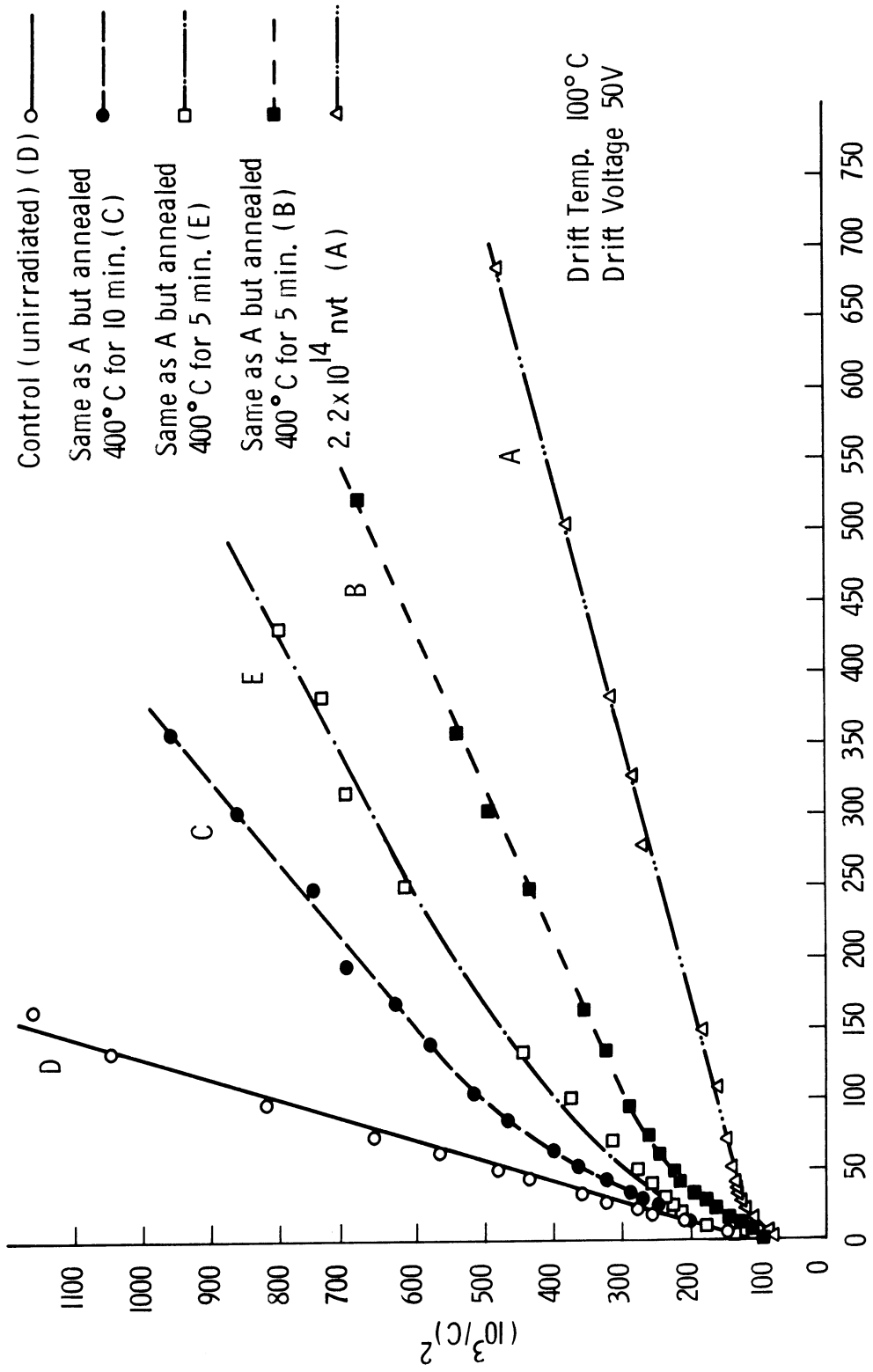

Fig. 12.--$(10^3/C)^2$ versus drift time for annealed neutron irradiated samples.

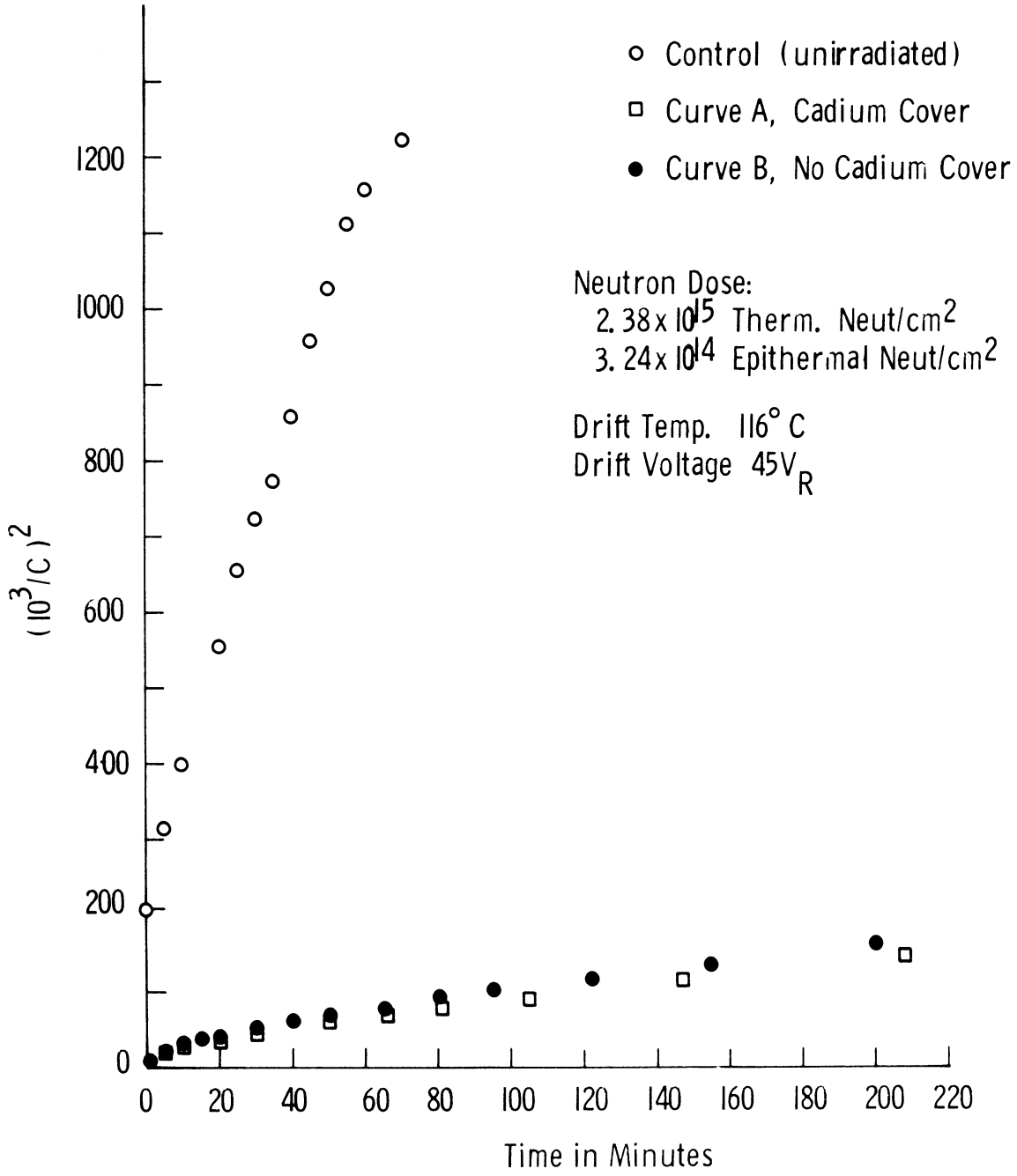

Fig. 13.--Relative effect of thermal and epithermal neutrons on lithium drift in silicon.

the two curves was observed. Consequently, the mobility of lithium in silicon appears to be dependent only on the fast neutron flux and possibly high energy gamma radiation present in the reactor.

In another study, junctions were exposed to eighty megarads of Co^{60} gammas and then drifted. No observable change in the performance of the diodes was found, so it appears that the primary effect on the diodes irradiated in the Ford Nuclear Reactor was due to epithermal neutrons.

For exposure to 1×10^{15} neutrons/cm^2 the junction capacitance fell to zero during irradiation and the diode could not be drifted. During intermediate exposure (3×10^{14} to 1×10^{15} neutrons/cm^2) the capacitance increased; however, this did not appear to affect the results of the subsequent drift. Nevertheless, exposures in which the capacitance of the junction increased were avoided, and were not used to determine the lithium mobility.

In the calculation of the lithium mobility and diffusion coefficient the assumption was made that the entire voltage placed across the diode was applied across the actual junction. This was verified by using

$$R = \frac{d\rho}{A} \qquad (5)$$

in which (ρ) denotes the resistivity of the material = 100 ohm-cm, (R) is the resistance of the sample, (A) is the area of the sample = 0.35 cm^2, and (d) represents the thickness of the sample = 0.15 cm. maximum.

Therefore, the maximum possible resistance of the bulk material in the diode is, from equation (5), 43 ohms. The current flowing through the diode under reverse bias was, at most, a few milliamperes giving 0.08 as the maximum voltage drop across the bulk p region. This is negligible compared to the reverse bias of 100 volts.

The change in resistivity of the p type material following neutron irradiation is also negligible. A study by Cleland, et al[4] demonstrates that no appreciable change in conductivity ($\sigma = 1/\rho$) occurs in p type silicon when the fast neutron flux is less than 1 x 10^{16} fast neutrons/cm^2. The maximum dose given to any sample in this work was 2.7 x 10^{14} neutrons/cm^2.

The results of the neutrons irradiation are summarized in Table 1 and Figure 14. A further discussion of the lithium-vacancy precipitate will be presented following the introduction of data from electron bombarded samples.

C. Lithium Mobility in Electron Bombarded Silicon

Typical results for lithium drifts in electron bombarded diodes are presented in Figures 15 and 16. Figure 15 illustrates the relative response of the electron bombarded samples with respect to an unirradiated sample, while Figure 16 is a representative plot from which the slope, $\frac{d}{dt}(10^3/C)^2$ was measured. Summary of the lithium diffusion coefficient is shown in Figure 17 and tabulated in Table 2.

The diodes could not be irradiated isotropically because the range of the 0.9 MeV electrons in silicon is 0.14 centimeters[5],

TABLE 1

LITHIUM DIFFUSION COEFFICIENT IN
NEUTRON IRRADIATED SILICON

Exposure # fast neut/cm^2	Lithium Diffusion Coefficient cm^2/sec	Temperature °C	Inverse Temperature $(°K)^{-1}$
1.1×10^{14}	2.59×10^{-14}	65	2.96×10^{-3}
1.1×10^{14}	7.23×10^{-14}	78	2.85×10^{-3}
1.1×10^{14}	3.86×10^{-13}	100	2.68×10^{-3}
2.4×10^{14}	1.03×10^{-14}	65	2.96×10^{-3}
2.4×10^{14}	3.24×10^{-14}	78	2.85×10^{-3}
2.4×10^{14}	1.61×10^{-13}	100	2.68×10^{-3}
2.4×10^{14}	1.53×10^{-12}	140	2.42×10^{-3}
2.7×10^{14}	6.41×10^{-15}	65	2.96×10^{-3}
2.7×10^{14}	2.42×10^{-14}	78	2.85×10^{-3}
2.7×10^{14}	1.09×10^{-12}	140	2.42×10^{-3}

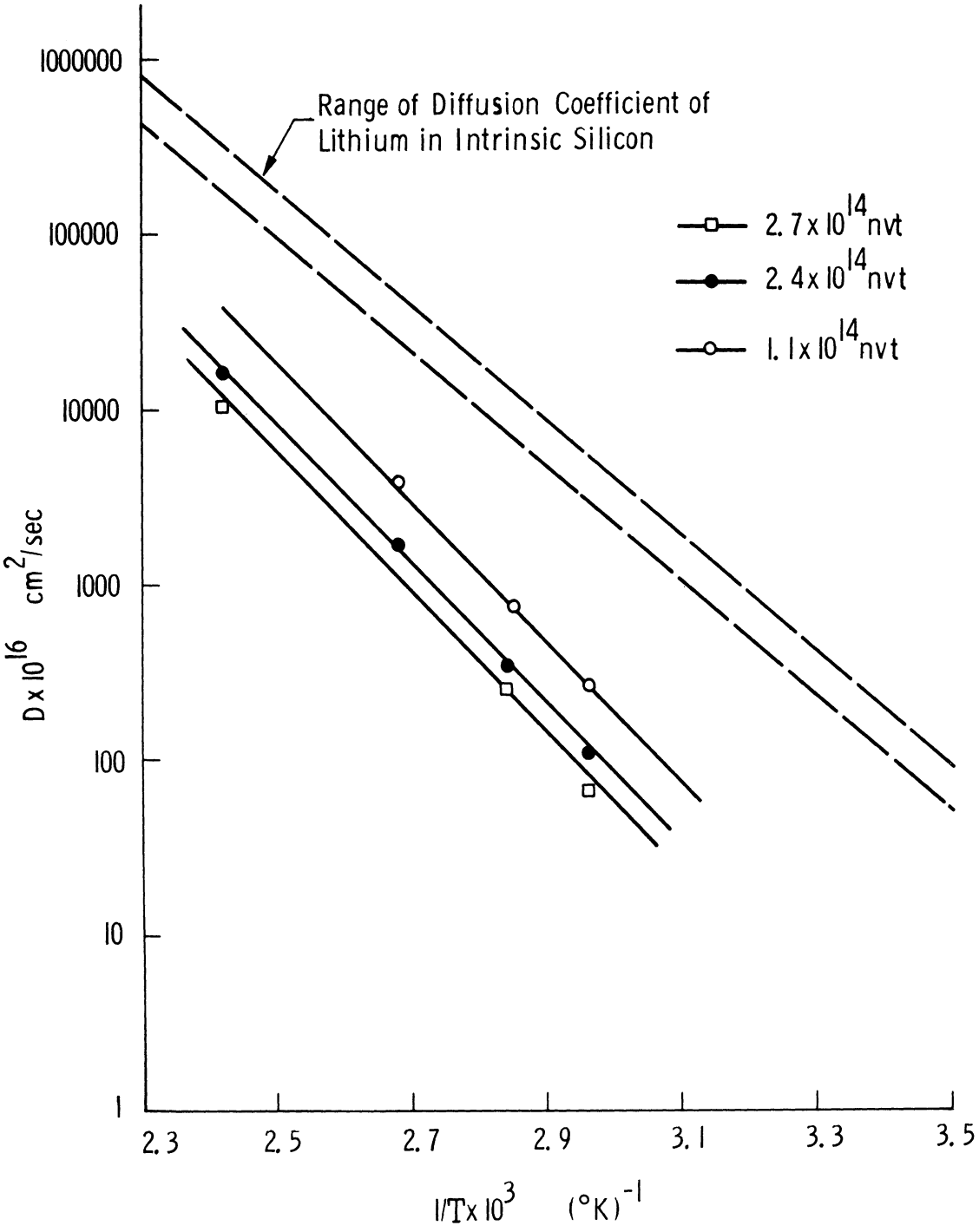

Fig. 14.--Effect of fast neutron bombardment on the diffusion coefficient of lithium in silicon.

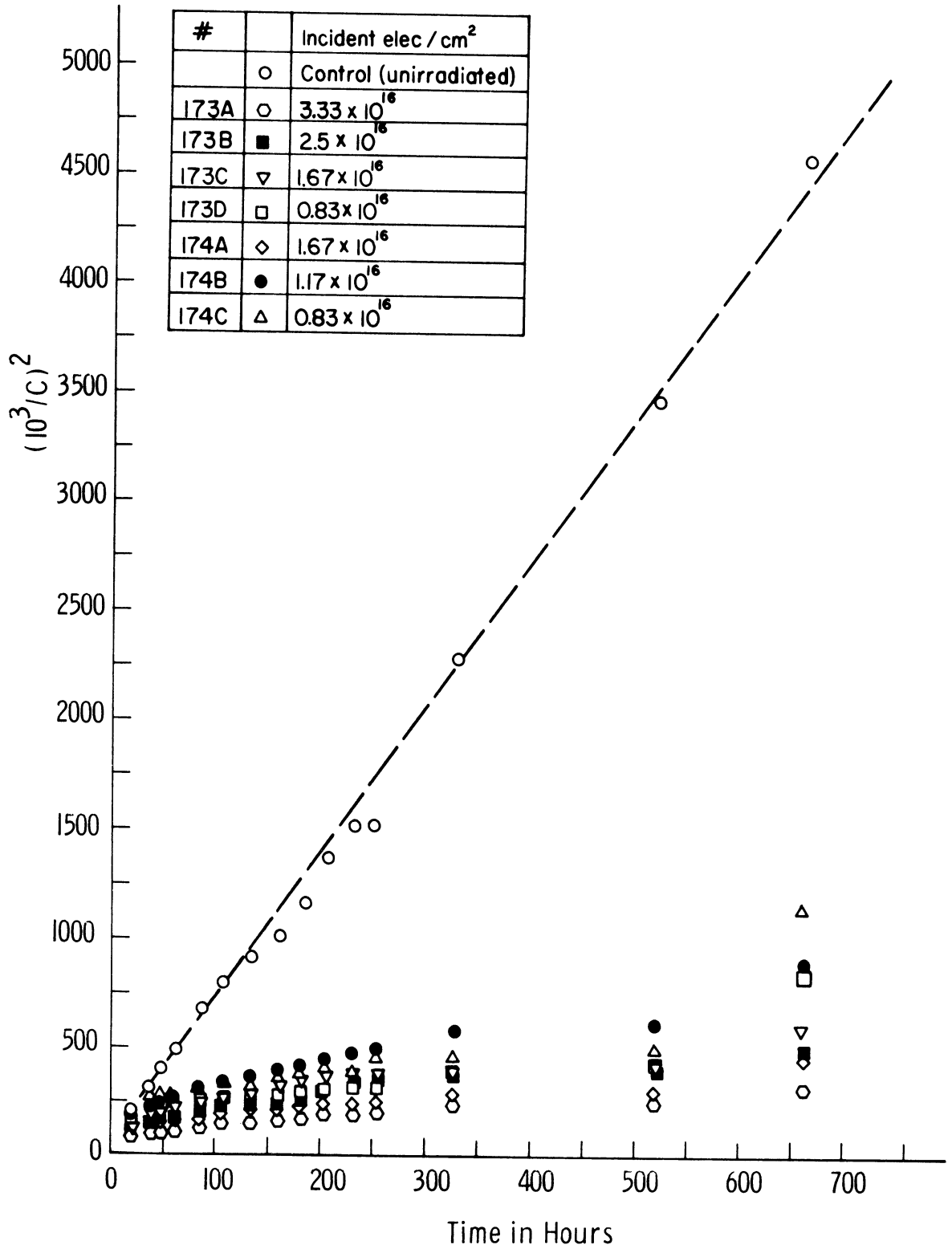

Fig. 15.--$(10^3/C)^2$ versus drift time for electron bombarded diodes.

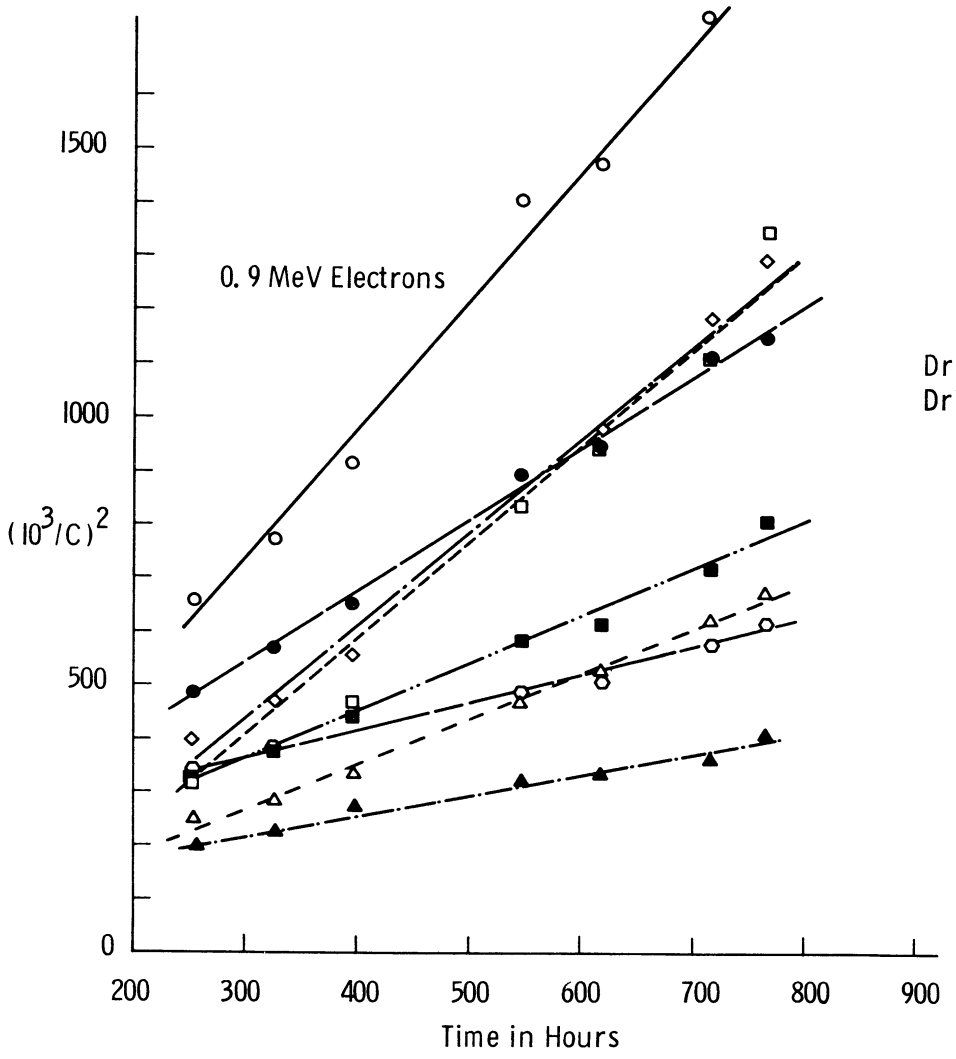

#174D ○
#173D □
#174C ◇
#174B ●
#173C ■
#174A △
#173B ○
#173A ▲

Drift Temp. 30° C
Drift Voltage $100V_R$

Data Obtained from Curves

#	$\Delta(10^3/C)^2$ 700-300 hr	slope hr^{-1}	slope sec^{-1}	W_{AVE} @T=500	Z/W_{AVE}
					$\times 10^4$
173A	152	0.380	1.056×10^{-4}	17.03	0.930
173B	210	0.525	1.458×10^{-4}	21.7	0.730
173C	353	0.883	2.453×10^{-4}	23.25	0.681
173D	712	1.780	4.944×10^{-4}	27.65	0.573
174A	332	0.830	2.306×10^{-4}	20.8	0.762
174B	530	1.325	3.313×10^{-4}	28.41	0.558
174C	695	1.738	4.828×10^{-4}	28.03	0.565
174D	955	2.388	6.633×10^{-4}	34.85	0.455

$Z = 1.584 \times 10^{-3}$ for 4 min. diffusion

Fig. 16.--$(10^3/C)^2$ versus drift time for electron bombarded diodes.

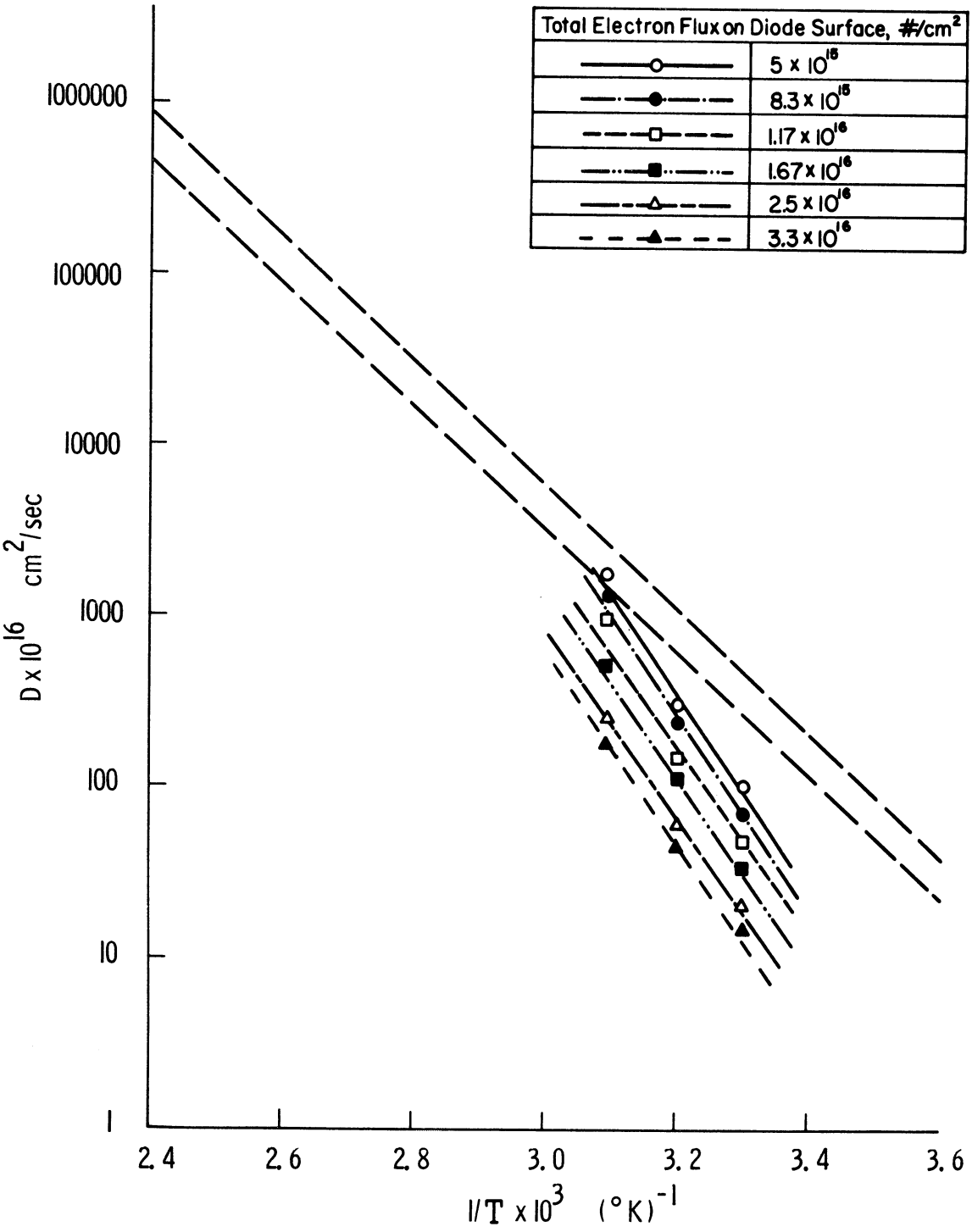

Fig. 17.--Effect of electron bombardment on the lithium diffusion coefficient in silicon.

TABLE 2

LITHIUM DIFFUSION COEFFICIENT IN
ELECTRON BOMBARDED SILICON

Electron Flux at Diode Surface #/cm^2	Relative Intensity Factor	Electron Flux in Junction #/cm^2	Average Diffusion Coefficient cm^2/sec	Inverse Temperature ($^\circ$K)$^{-1}$
5.0×10^{15}	0.93	4.65×10^{15}	1.0×10^{-14}	3.3×10^{-3}
8.3×10^{15}	0.93	7.73×10^{15}	7.0×10^{-15}	"
1.17×10^{16}	0.93	1.09×10^{16}	4.63×10^{-15}	"
1.67×10^{16}	0.93	1.55×10^{16}	3.24×10^{-15}	"
2.5×10^{16}	0.93	2.33×10^{16}	1.94×10^{-15}	"
3.33×10^{16}	0.93	3.10×10^{16}	1.32×10^{-15}	"
5.0×10^{15}	0.92	4.60×10^{15}	3.02×10^{-14}	3.2×10^{-3}
8.3×10^{15}	0.92	7.64×10^{16}	2.33×10^{-14}	"
1.17×10^{16}	0.92	1.08×10^{16}	1.37×10^{-14}	"
1.67×10^{16}	0.92	1.53×10^{16}	1.15×10^{-14}	"
2.5×10^{16}	0.93	2.33×10^{16}	5.70×10^{-15}	"
3.33×10^{16}	0.93	3.10×10^{16}	4.32×10^{-15}	"
5.0×10^{15}	0.90	4.50×10^{15}	1.71×10^{-13}	3.09×10^{-3}
8.3×10^{15}	0.91	7.55×10^{15}	1.32×10^{-13}	"
1.17×10^{16}	0.91	1.06×10^{16}	9.60×10^{-14}	"
1.67×10^{16}	0.92	1.53×10^{16}	5.09×10^{-14}	"
2.5×10^{16}	0.93	2.33×10^{16}	2.39×10^{-14}	"
3.33×10^{16}	0.93	3.10×10^{16}	1.77×10^{-14}	"

equivalent to the sample thickness. Because the diodes were bombarded on the n-side the lithium drifted into an area of diminished electron exposure. This effect was compensated by determining the average depth of the lithium penetration and then finding the relative intensity factor, (I/I_o), from a range-energy curve.[5] The relative intensity factor is tabulated in Table 2, along with the electron flux incident on the surface of the sample, I_o. The minimum relative intensity factor was 0.90 which corresponded to an average lithium penetration of 0.015 centimeters. The corrected electron flux will be used in the following analysis of the lithium-vacancy precipitate.

D. Analysis of the Lithium-Vacancy Precipitate

This section presents evidence that the lithium is precipitated at the vacancy site rather than pairing with the vacancy. The precipitate behaves as an insoluble salt in silicon and is in equilibrium with the lithium ion and the ionized vacancy.

A hypothetical lithium-vacancy pair would have the following dissociation and equilibrium relations as developed in Chapter II.

$$P \rightleftharpoons Li^{+} + D^{-} \tag{6}$$

$$\frac{P/N}{[\,1 - P/N\,]^2} = NK_p \tag{7}$$

The quantity P/N can be calculated from experimentally determined values of the lithium diffusion coefficient.

$$P/N = 1 - D/D^{o} \tag{8}$$

In the above equation (D) represents the diffusion coefficient in irradiated silicon and (D°) denotes the diffusion coefficient in intrinsic silicon.

To evaluate equation (7), the quantity $\frac{P/N}{(1 - P/N)}2$ is plotted versus (N) for a constant temperature. Although the number of vacancy sites, N, is unknown, it is equal to a constant times the incident electron or neutron flux.[8]

$$N = \xi_E N_E \tag{9}$$

or

$$N = \xi_N N_N \tag{10}$$

Because K_p is a constant, $\frac{P/N}{(1 - P/N)}2$ must be a linear function of N_E or N_N. As is illustrated in Figure 18 and Table 3, a plot of $\frac{P/N}{(1 - P/N)}2$ versus N_E is not a straight line, hence, $\xi_E K_p$ is not a constant and the theory of pairing does not correctly describe the lithium-vacancy interaction. This result is confirmed by calculating the distance of closest approach, (a), of the hypothetical pair from equation (II-40).

$$P/N = 4\pi\xi_E N_E \int_a^r r^2 \exp[q^2/kkTr]\, dr \tag{II-40}$$

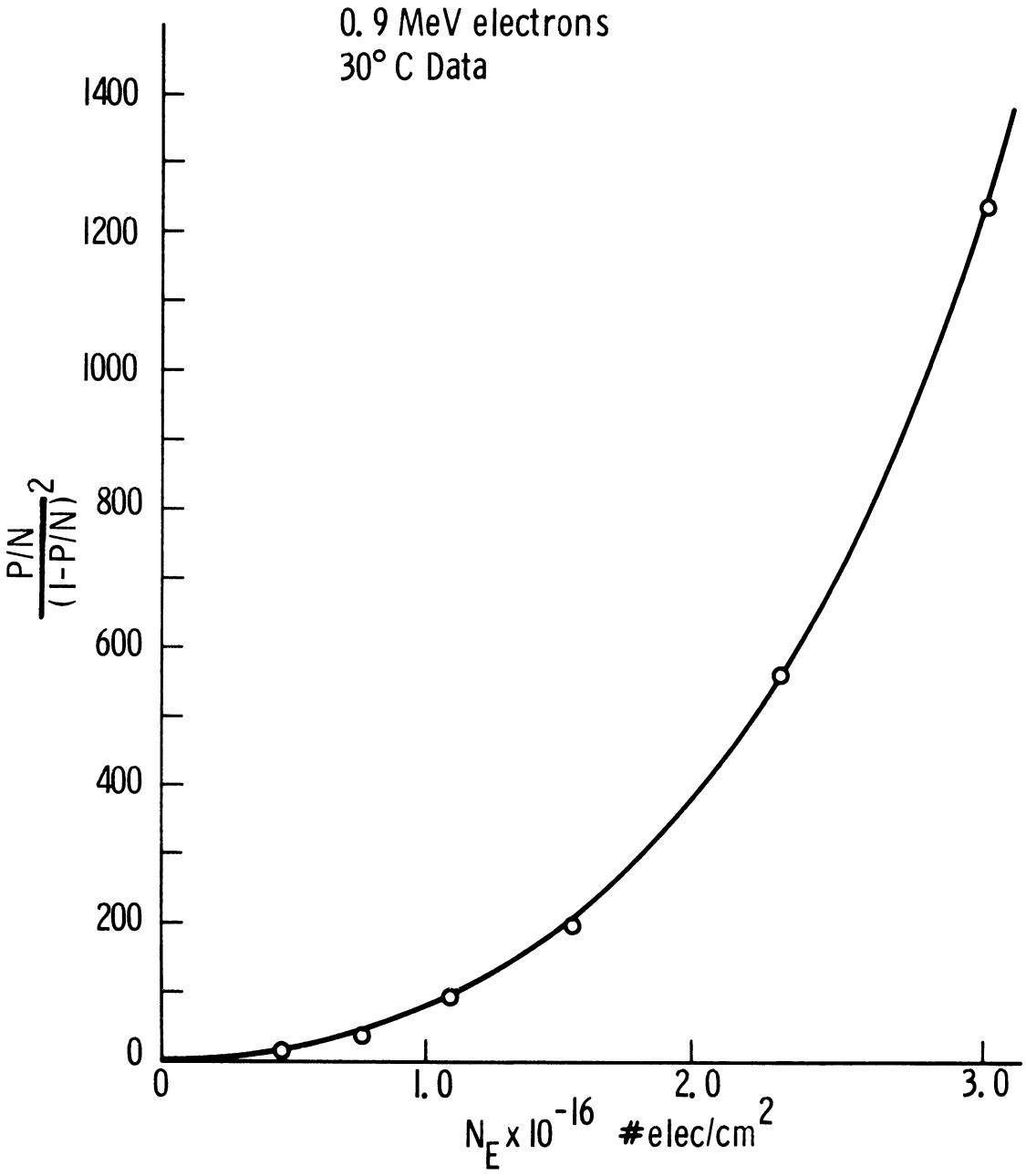

Fig. 18.--A plot of $\frac{P/N}{(1 - P/N)}2$ versus N_E.

TABLE 3

CALCULATIONS FOR THE ION PAIR MODEL:

$$\frac{P/N}{(1 - P/N)^2} = N_E \xi_E K_P$$

Temperature: 30°C
Electron bombarded samples
$D^\circ_{30} = 4.7 \times 10^{-14}$ cm^2/sec.

Electron Flux, N_E #/cm^2	$D/D^\circ = (1 - P/N)$	P/N	$\frac{P/N}{(1 - P/N)^2}$
4.65×10^{15}	0.213	0.787	17.4
7.73×10^{15}	0.149	0.851	38.3
1.09×10^{16}	0.0985	0.9014	92.8
1.55×10^{16}	0.069	0.931	195.1
2.33×10^{16}	0.0413	0.9587	560.0
3.10×10^{16}	0.0281	0.9719	1240.0

Assuming arbitrary values of ξ_E from one to ten, and using the data for the electron irradiated silicon samples, calculations with equation (II-40) produces values of (a) between 2.6 and 15 Å. These excessively large values indicate that the expressions for ion pairing do not apply to the lithium-vacancy interaction.

In addition to the simple model of ion pairing in which the pair is formed with one lithium and one vacancy, the following more complex dissociation models were calculated and found unsatisfactory:

$$P \rightleftarrows 2Li^+ + 2D^-$$

$$P \rightleftarrows 2Li^+ + D^=$$

$$P \rightleftarrows Li^+ + D^-$$

$$\downarrow\uparrow$$

$$D^= + Li^+$$

In the last model listed above, each defect is considered doubly ionized and pairs with lithium with two different equilibrium constants.

Considering the lithium-vacancy precipitate as an insoluble salt, as discussed in Chapter II, the following expressions describe the relationship between the solute and the lithium ions.

$$S \rightleftarrows Li^+ + D^- \tag{11}$$

$$[\, 1 - S/N \,] = K_S'/N \tag{12}$$

The quantity S/N can be calculated from experimentally determined values of the lithium diffusion coefficient.

$$S/N = [\, 1 - D/D^{o} \,] \tag{13}$$

To determine whether or not lithium precipitates at a vacancy site, (1 - S/N) versus 1/N is plotted for a constant temperature. As noted previously, $N = \xi_E N_E$ or $= \xi_N N_N$. Because K_s' is a constant, (1 - S/N) must be a linear function of $1/N_E$ or $1/N_N$. As is illustrated in Figure 19 and Table 4, a plot of (1 - S/N) versus $1/N_E$ is a straight line. It can then be concluded that the lithium precipitates at the vacancy site.

Results from all the neutron and electron irradiated samples are displayed in Figure 20. The lithium was drifted in the electron irradiated diodes in the following sequence: 30°C, 40°C, and 50°C. The junction capacitances ranged from below 20 pf during the 50°C drift to above 50 pf during the 30°C drift. Difficulty in obtaining accurate measurement of capacitances below 20 pf was responsible for the scatter in the data between 40°C and 50°C displayed in Figure 20.

Quantitative measurements cannot be made for the number of vacancies produced per incident radiation; however, the relative effect of neutron and electron irradiation can be determined from the amount of radiation necessary to decrease the lithium diffusion coefficient to the same value at a given temperature. From Figures 14 and 17, it can be seen that at 30°C ($1/T = 3.3 \times 10^{-3}$) the diffusion coefficient is the same for a dose of 1.1×10^{14} fast neutrons or 3.3×10^{16} electrons.

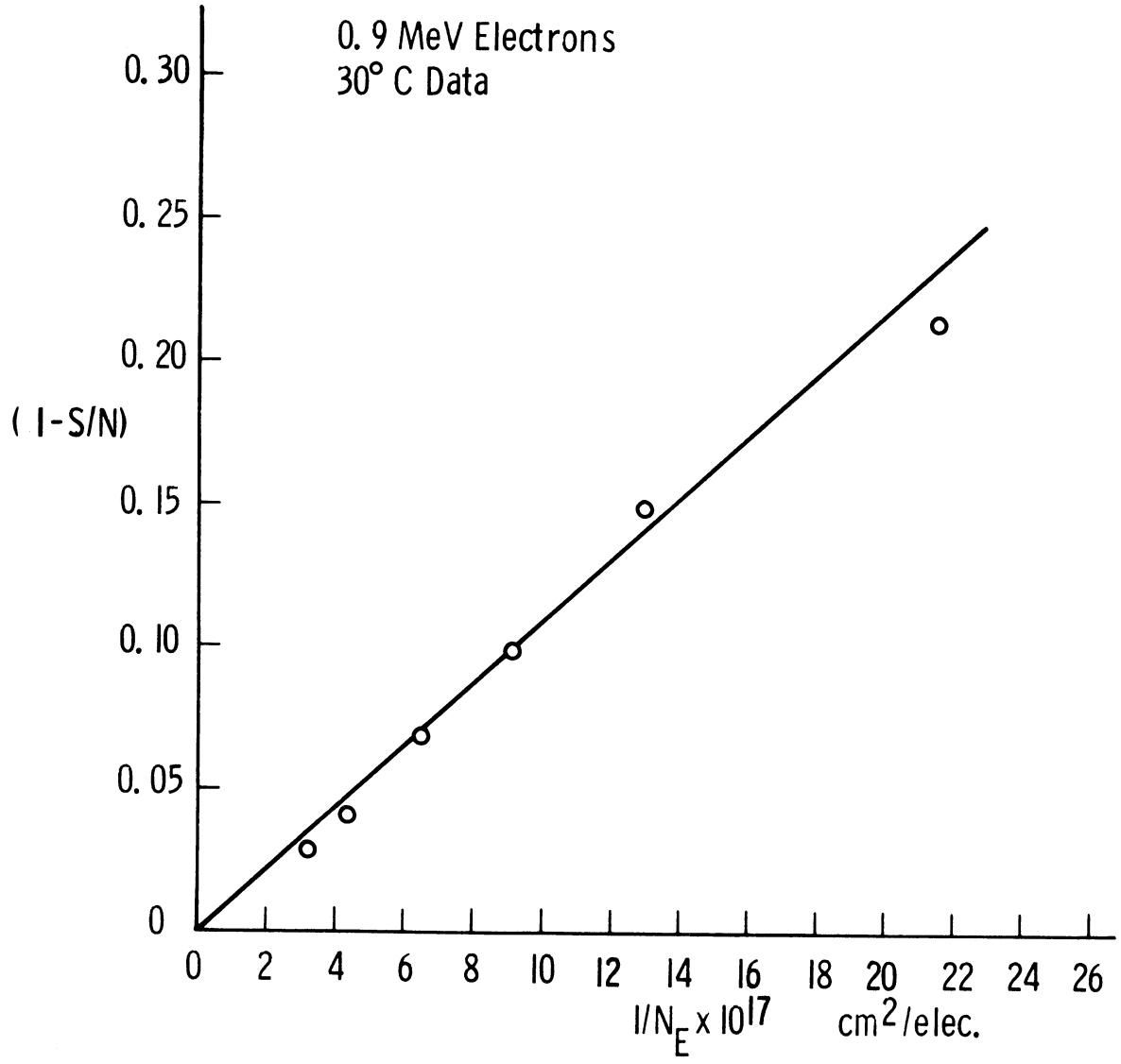

Fig. 19.--A plot of (1 - S/N) versus $1/N_E$.

TABLE 4

CALCULATIONS FOR LITHIUM-VACANCY PRECIPITATION:
$(1 - S/N) = K_S' / \xi_E N_E$

Temperature: 30°C
Electron bombarded samples
$D_{30}^{\circ} = 4.7 \times 10^{-14}$ cm^2/sec.

Electron Flux, N_E #/cm^2	$1/N_E$ cm^2/#	D/D° $(1 - S/N)$
4.65×10^{15}	21.5×10^{-17}	0.213
7.73×10^{15}	12.9×10^{-17}	0.149
1.09×10^{16}	9.2×10^{-17}	0.0985
1.55×10^{16}	6.5×10^{-17}	0.069
2.33×10^{16}	4.3×10^{-17}	0.0413
3.10×10^{16}	3.2×10^{-17}	0.0281

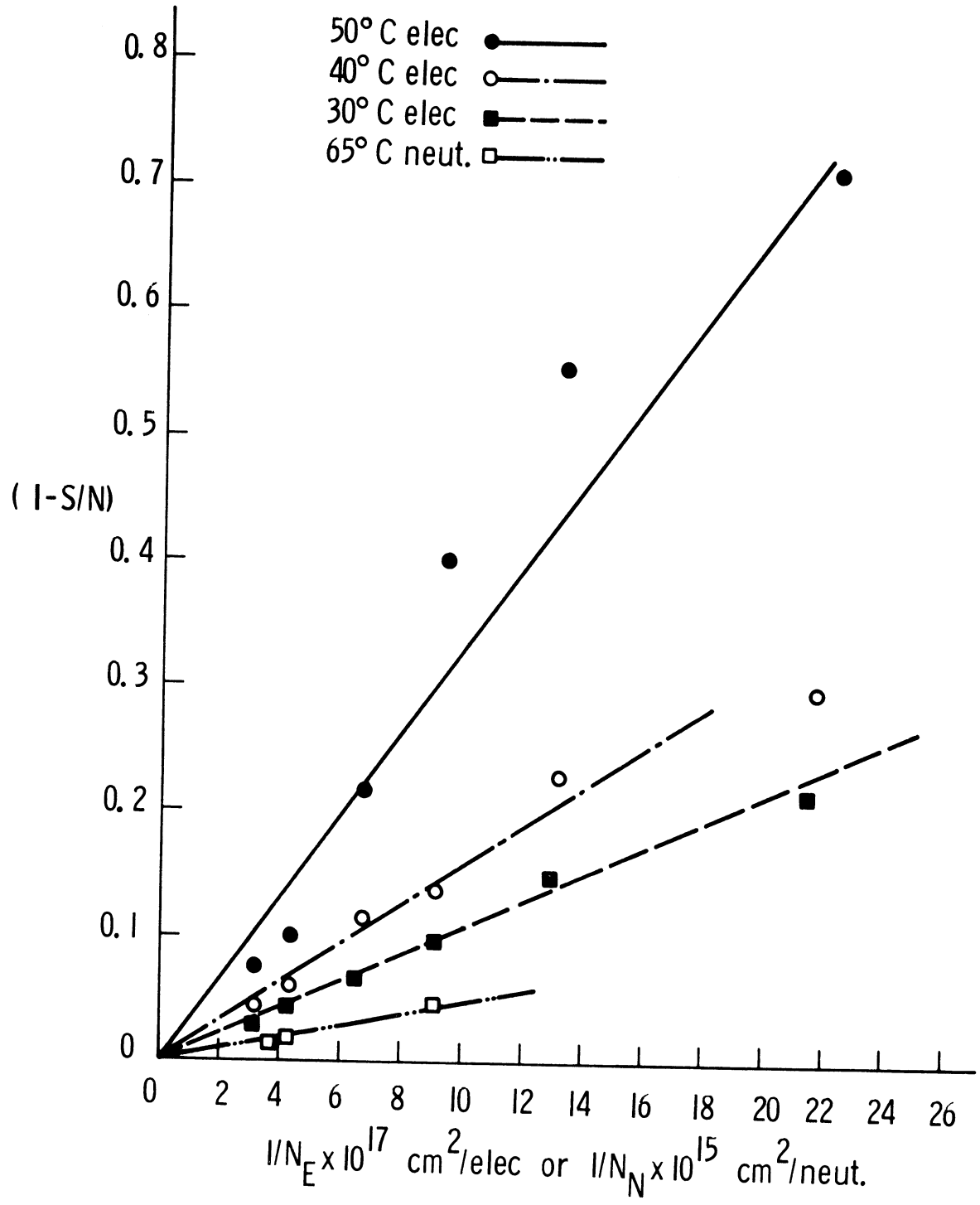

Fig. 20.--A plot of (1 - S/N) versus $1/N_E$ or $1/N_N$ for all data.

$$D_{30} = D_{30}^{o}(1 - S/N) = \left.\frac{D_{30}^{o} K_s'}{\xi_E N_E}\right|_{N_E = 3.3\times10^{6}} = \left.\frac{D_{30}^{o} K_s'}{\xi_N N_N}\right|_{N_N = 1.1\times10^{14}} \quad (14)$$

$$\frac{\xi_N}{\xi_E} = \frac{N_E}{N_N} = \frac{3.3 \times 10^{16}}{1.1 \times 10^{14}} \quad (15)$$

$$\frac{\xi_N}{\xi_E} = 300 \quad (16)$$

The ratio of the number of defects produced per incident fast neutron, ξ_N, to the number of defects produced per incident 0.9 MeV electron, ξ_E, is, from radiation damage theory,

$$\frac{\xi_N}{\xi_E} = \frac{N_N / \Phi_N t_N}{N_E / \Phi_E t_E} = \frac{N_{Si}\,\sigma_N\,\nu_N}{N_{Si}\,\sigma_E\,\nu_E} = \frac{\sigma_N\,\nu_N}{\sigma_E\,\nu_E} \quad (17)$$

In equation (17), N_N represents the number of defects produced by fast neutron irradiation, Φ_N is the fast neutron flux, and t_N denotes the reactor exposure time. Similarly, N_E, represents the number of defects produced by 0.9 MeV electron bombardment, Φ_E, is the electron flux, and t_E is the length of the electron bombardment. The quantity N_{Si} is the number of silicon atoms/cm^3 and σ_N and σ_E

denote the cross section for displacement for fast neutrons and 0.9 MeV electrons in silicon. Finally, ν_N is the number of displacements produced in the silicon per neutron interaction, and ν_E is the number of displacements produced in silicon per electron interaction.

The fast neutron displacement cross section has been experimentally determined to be 1.7 barns,[6] and the displacement cross section for 0.9 MeV electrons can be calculated from the expression below.[7]

$$\sigma_E = 4\pi a_H^2 Z_1^2 Z_2^2 \frac{M_1}{M_2} \frac{I_H^2}{E_1 E_d} \tag{18}$$

The nomenclature for this relation is as follows:

a_H is the Bohr radius.

Z_1 is the charge of the electron in units of (1.6×10^{-19} coul.).

Z_2 is the charge of the silicon nucleus.

M_1 is the mass of the electron.

M_2 is the mass of the silicon atom.

I_H is the ionization energy of hydrogen.

E_1 is the energy of the incident electron.

E_d is the displacement energy in silicon. E_d = 25 ev.

The quantity σ_E calculated from equation (18) for 0.9 MeV electrons in silicon is 11.2 barns.

The number of displacements produced in silicon per neutron interaction can be calculated from the expressions,[8]

$$\nu_N = \bar{T}_m / 2E_d$$

$$\bar{T}_m = \frac{4}{A}(0.58) \qquad (19)$$

In the above expressions, $\bar{T}_m$ is the mean energy of the primary knock-on silicon atom, and A is the atomic mass of silicon. Calculated values for ν_N and $\bar{T}_m$ are 1660 and 83 KeV, respectively.

Finally, ν_E can be determined from the relation,[8]

$$\nu_E = \frac{1}{2}\left[\frac{\bar{T}_m}{\bar{T}_m - E_d}\right]\left(1 + \mathrm{Ln}(\bar{T}_m/2E_d)\right) \qquad (20)$$

For electrons, $\bar{T}_m$ is,[8]

$$\bar{T}_m = \frac{2\left[E_1 + 2M_1c^2\right]E_1}{M_2c^2} \qquad (21)$$

Using equations (20) and (21), calculations show that $\nu_E = 1.2$ and $\bar{T}_m = 125$ ev for 0.9 MeV electrons in silicon.

Inserting the values calculated from expressions (18) to (21) into equation (17), the ratio ξ_N/ξ_E can be determined.

$$\xi_N/\xi_E = \frac{\sigma_N \nu_N}{\sigma_E \nu_E} = \frac{1.7 \times 1660}{11.2 \times 1.2} = 210 \qquad (22)$$

This quantity, based on radiation damage theory, is in reasonable agreement with experiment. Compare equation (22) to equation (16).

CHAPTER V

CONCLUSIONS

Investigations reported in this study indicate that the mobility and diffusion properties of lithium in single crystal silicon are critically dependent on the number of radiation induced vacancies. Moreover, the lithium is precipitated at defect sites rather than becoming paired to vacancies. Lithium precipitate is atomic; however, a paired lithium is an ion.

The mobility of lithium in irradiated silicon was drastically reduced because of the precipitation of the lithium at immobile vacancy sites. The effective lithium diffusion coefficients in irradiated silicon are shown in Table 5.

The diffusion coefficient in irradiated silicon is inversely proportional to the dose. The diffusion coefficient in boron doped silicon is dependent on $(N_B)^{-1/2}$ due to the formation of ion pairs.[1] Table 5 reveals that (D) is more temperature dependent (larger negative exponential coefficients) in irradiated and boron doped silicon than in intrinsic silicon. This can be explained as follows: Lithium diffused into intrinsic silicon forms no pairs and does not precipitate so the amount free to move is constant. Lithium diffused into irradiated or boron doped silicon forms pairs and precipitates, hence, the amount of

TABLE 5

LITHIUM DIFFUSION COEFFICIENTS IN IRRADIATED SILICON

Type of Silicon	D cm^2/sec	Dose $\#/cm^2$	Boron Conc. $\#/cm^3$	Temp. Range °K
Intrinsic[2]	$2.3 \times 10^{-3}\ e^{-0.66/kT}$	--	--	300-400
Boron Doped[1]	$\frac{3.0 \times 10^{8}}{N_B^{\frac{1}{2}}}\ e^{-0.80/kT}$	--	1×10^{14} to 1×10^{17}	275-333
Fast Neutron Irradiated*	$\frac{7.0 \times 10^{12}}{N_N}\ e^{-0.83/kT}$	1×10^{14} to 3×10^{14}	below 1×10^{14}	300-410
Electron Irradiated (0.9 MeV)	$\frac{2.1 \times 10^{18}}{N_E}\ e^{-1.03/kT}$	1×10^{16} to 2×10^{18}	below 1×10^{14}	300-330

*Thermal neutron irradiation does not alter the diffusion properties of lithium in silicon.

lithium ions free to move is equilibrium with the pairs or precipitate. The equilibrium concentrations are temperature dependent, consequently, the diffusion coefficient in silicon where pairs or precipitates are present has increased temperature dependence.

The effective lithium diffusion coefficient for electron bombarded silicon has greater temperature dependence than neutron irradiated crystals. This can be explained in the following manner. Wertheim has shown that in electron irradiated silicon the interstitial will not be driven more than a few atomic distances away from its parent vacancy during a primary collision for most energy transfers.[3] The lithium ion experiences a dipole effect and the lithium precipitate is under the influence of the nearby interstitial, consequently, its interaction strength may be weakened. If this is the case, the precipitate will be less stable, hence the effective lithium diffusion coefficient will have a greater temperature dependence. This phenomena does not occur with neutron irradiated samples because the interstitials are driven far from the vacancies. Clustering occurs; however, the average distance between the interstitial and the vacancy will be large compared to the separation of the Frenkel pair created by electron bombardment.

The drifting characteristics of lithium in irradiated diodes was drastically altered. Evidence that the lithium moved during irradiation was displayed by the large initial slope of the drift curves. Initially, the rate of decrease of the junction capacitance is the same for irradiated as it is for intrinsic silicon. This indicated that the lithium precipitated at the vacancies in the junction region produced an

intrinsic zone. However, as the lithium drifts out of the junction, its mobility is governed by the number of defects produced in the bulk silicon, and the slope of the drift curve decreased to a constant but lower value. The action described above occurs with both electron and neutron irradiated diodes. No change in the drift characteristics was experienced by diodes irradiated with Co^{60} gammas.

An annealing study eliminated the possibility that the change in the effective mobility of lithium was caused by an anomalous junction effect. Reheating the diodes after irradiation caused the lithium to move farther into the crystal thereby establishing a new junction. Because the drifting properties of the newly formed junction were identical to unheated diodes, the cause of the altered drift characteristics was ascribed to defects produced in the bulk region of the crystal.

The results of conductivity measurements indicated that the irradiation does not alter the resistivity of the bulk silicon sufficiently to affect the drift measurements.

The measurement of the lithium mobility in irradiated silicon does not offer quantitative information about the number of defects produced per incident, fast neutron or electron. The information provided by these measurements does, however, allow a relative measure of the vacancies produced by fast neutrons and electrons. The number of vacancies produced per incident fast neutron divided by the number of vacancies produced per incident 0.9 MeV electron was found to be 300. This is in reasonable agreement with a value of 210 calculated employing radiation damage theory.

The primary purpose of this study was to investigate the motion of lithium in irradiated silicon. However, it has some practical significance.

The widely used lithium drift detectors are slowly damaged by the same radiation they are employed to detect. The constant bombardment of electrons and neutrons in the detectors produce defects in the space charge region and the subsequent rearrangement of lithium reduces the detector resolution. Because of the stability of the lithium-vacancy precipitate, the sensitive junction area can be rejuvenated by redrifting the damaged detectors.[4]

It was thought that during the redrift process the defects annealed. Silicon defects do not anneal appreciably below 200°C; therefore, annealing of defects during redrift at 150°C is unlikely. This study shows that, during the redrift of damaged detectors, lithium precipitates at vacancy sites creating neutral complexes which are stable and do not disturb the space charge region.

The lithium mobility is reduced in the redrifted junction. This may cause the redrifted detector to be more stable and less susceptible to radiation damage than a new detector because the rearrangement of the lithium takes place at a slower rate. In fact, it may be possible to create many other radiation resistant semiconductor devices by employing irradiated silicon and lithium.

APPENDIX A

QUANTITATIVE DESCRIPTION OF THE SEMICONDUCTOR WATER ANALOGY[1]

The equilibrium relation for the hydrolysis of water is,

$$[H^+]\ [OH^-] = K = 10^{-14} \text{ (mole/liter)}^2 \quad (1)$$

For pure water $[H^+]$ equals $[OH^-]$,

$$[H^+] = [OH^-] = 10^{-7} \text{ (moles/liter)} \quad (2)$$

Because one mole equals 6.03×10^{23} ions, equation (2) is

$$[H^+] = 6.03 \times 10^{13} \text{ (ions/liter)} \quad (3)$$

The enthalpy change, ΔH, for the hydrolysis is 13,300 Kcal/mole at 300°K. This quantity can be expressed in terms of ev/ion by using the conversion factor one ev/molecule = 23.05 Kcal/mole. So ΔH for the hydrolysis is,

$$\frac{\Delta H}{N_o} = 0.58 \text{ ev/ion} \quad (4)$$

For pure silicon the corresponding equilibrium relation for electron-hole recombination and generation is

$$[e^+]\ [e^-] = K = 1.4 \times 10^{26} \text{ (elec/liter)}^2$$

or

$$[e^+]\ [e^-] = K = 4 \times 10^{-22} \text{ (mole/liter)}^2$$

$$[e^+] = 1.2 \times 10^{13} \quad \text{elec/liter}$$

or

$$[e^+] = 2 \times 10^{-11} \quad \text{mole/liter}$$

The enthalpy change ΔH per electron or hole is equal to the band gap, 1.1 ev. In terms of Kcal/mole this is,

$$\frac{\Delta H}{N_o} = 25.2 \quad \text{Kcal/mole}$$

The values calculated above are presented in Table 6 with values for germanium and water.

TABLE 6

COMPARISON OF SILICON AND GERMANIUM TO WATER

	Silicon	Germanium	Water
Positive ion or hole	$[e^+]$	$[e^+]$	$[H^+]$
Negative ion or electron	$[e^-]$	$[e^-]$	$[OH^-]$
Ion product (moles/liter)^2	4×10^{-22}	2.2×10^{-15}	1×10^{-14}
Concentration of ion or hole in pure material	2×10^{-11}	4.7×10^{-8}	1×10^{-7}
Acid condition	p-type boron doped	p-type boron doped	$HC_2H_3O_2$
Basic condition	n-type phosphorus doped	n-type phosphorus doped	NH_4OH
ΔH (Kcal/mole)	25.2	16.6	13.3
ΔH (ev/ion)	1.1	0.72	0.58
ϵ, dielectric constant	12	16	80

APPENDIX B

SAMPLE CALCULATIONS

Equation (II-83) gives the lithium mobility in terms of the slope of the drift curve, $\frac{d}{dt}(10^3/C)^2$.

$$\mu = X\left[\frac{X - Z/W_A}{2V}\right] \frac{d}{dt}(10^3/C)^2 \qquad (1)$$

C = junction capacitance (pf)

Z = $2D_o t_o/x_o$ (cm/sec)

V = reverse bias (volts)

W_A = average width of junction expressed in units of $10^3/C$

X = $K \epsilon A \times 10^3 = 1.062A \times 10^{-3}$, A in cm^2

$K\epsilon$ = 1.062×10^{-10} $coul^2/n\text{-}m^2$

$\frac{d}{dt}(10^3/C)^2$ = slope of drift curve $1/pf^2 - sec^2$

D_o = lithium diffusion coefficient in silicon at 420°C

t_o = diffusion time

x_o = distance from surface of crystal to junction. This is the point where $N_{Li} = N_B$ as shown in Figure 3.

The distance from the surface of the crystal to the junction, x_o, must be calculated in order to find Z. The quantity (x_o) can be found from equation (II-59),

$$N_{Li} = N_o \text{ erfc } [x/2(D_o t_o)^{\frac{1}{2}}] \qquad (2)$$

by applying the expansion

$$\text{erfc } x \cong \frac{e^{-x^2}}{x\sqrt{\pi}} - \frac{e^{-x^2}}{2x^3\sqrt{\pi}} \cdots\cdots\cdots \quad (3)$$

$$N_{Li} = \frac{2(D_o t_o)^{\frac{1}{2}}}{x\sqrt{\pi}} N_o \, e^{-x^2/4D_o t_o} \quad (4)$$

In the above equation, N_o is the number of lithium atoms per cm^3 at the surface of the crystal. At x_o, $N_{Li} = N_B$.

$$\frac{x_o\sqrt{\pi}}{2(D_o t_o)^{\frac{1}{2}}} \frac{N_B}{N_o} = e^{-x_o^2/4D_o t_o} \quad (5)$$

The logarithm of equation (5) is

$$\text{Ln}\left(\frac{x_o\sqrt{\pi}}{2(D_o t_o)^{\frac{1}{2}}}\right) + \text{Ln}\,(N_B/N_o) = -\frac{x_o^2}{4D_o t_o} \quad (6)$$

Let J be the quantity, $x_o/2(D_o t_o)^{1/2}$

$$J^2 + \text{Ln } J + \text{Ln}\,(N_B\pi/N_o) = 0 \quad (7)$$

For 100 ohm-cm silicon $N_B = 1.6 \times 10^{14}$ boron atoms/cm^3 and N_o is equal to 1×10^{18} lithium atoms/cm^3.[1] Trial and error solution of equation (7) with the above values for N_B and N_{Li} yields a value of 2.60 for J.

The quantity, (Z), is

$$Z = 2D_o t_o/x_o = (D_o t_o)^{\frac{1}{2}}/J \quad (8)$$

For D_o equal to 0.405×10^{-7} cm^2/sec at 420°C, [2] and t_o equal to four minutes, (Z) is 1.58×10^{-3} cm/sec.

A sample calculation can now be performed with equation (II-83) using the data from diode #173A (see Figure 16).

$$\mu = \frac{X\,(X - Z/W_A)}{2V} \frac{d}{dt}(10^3/C)^2$$

1) Area in cm^2 A, 0.3385
2) $X = 1.062 \times 10^{-3} \times 0.3385 = 0.3595 \times 10^{-3}$
3) Slope of drift curve (Figure 16) = 1.056×10^{-4} sec^{-1}
4) Average $W = W_{ave} = W_A$ (between 300 and 700 hours) = $(10^3/C)^2$ at 500 hours = 17.03
5) $Z/W_A = 1.58 \times 10^{-3}/17.03 = 0.93 \times 10^{-4}$
6) Reverse bias, V = 100 volts

$$\mu = \frac{3.595(3.595 - 0.930) \times 10^{-8} \times 1.056 \times 10^{-4}}{2 \times 10^2}$$

$$\mu = 5.05 \times 10^{-14} \text{ cm}^2/\text{volt-sec.}$$

The diffusion coefficient is found from the Einstein relation,

$$D = \frac{\mu kT}{e}$$

For diode #173A drifted at 30°C,

$$D = \frac{5.05 \times 10^{-4}(1.38 \times 10^{-23})(3.03 \times 10^2)}{1.6 \times 10^{-19}}$$

$$D = 1.32 \times 10^{-15} \text{ cm}^2/\text{sec.}$$

BIBLIOGRAPHY

Chapter I:

1. Pell, E. M., "Ion Drift in an n-p Junction," J. Appl. Phys. 31, 291 (1960).

2. Lehrer, F. A. and Reiss, H., "Details of Ion Drift in an n-p Junction," J. Appl. Phys. 33, 2353 (1962).

3. Ammerlaan, C. A. J. and Ulder, K., "The Preparation of Lithium-Drifted Semiconductor Nuclear Particle Detectors," Nucl. Inst. Methods 21, 97 (1963).

4. Baily, N. A. and Hilbert, J. W., "The Response of p-i-n Junctions to Beta Rays," Phys. Med. Biol. 10, 42 (1965).

5. Blankenship, J. L. and Borkowski, C. J., "Improved Techniques for Producing p-i-n Diode Detectors," IRE Trans. Nucl. Sci. NS-9, No. 3, 181 (1962).

6. Elliott, J. H., "Thick Junction Radiation Detectors Made by Ion Drift," Nucl. Instr. Methods 12, 60 (1961).

7. Gibbons, P. E., "On the Design of a Silicon Junction Radiation Detector Made by Ion Drift," Nucl. Instr. Methods 16, 284 (1962).

8. Mann, H. M., Haslett, J. W. and Janarek, F. J., "Lithium-Drifted p-i-n Junction Detectors," IRE Trans. Nucl. Sci. NS-9, No. 4, 43 (1962).

9. Miller, G. L., Pate, B. D. and Wagner, S., "Production of Thick Semiconductor Radiation Detectors by Lithium Drifting," IEEE Trans. Nucl. Sci. NS-10, No. 1, 220 (1963).

10. Coleman, J. A. and Rodgers, J. W., "Radiation Damage in Lithium Drifted p-i-n Junctions," IEEE Trans. Nucl. Sci. NS-11, No. 3, 213 (1964).

11. Dearnaley, G., "Radiation Damage Effects in Semiconductor Detectors," Nucleonics 22, No. 7, 78 (1964).

12. Scott, R. E., "Radiation Effects of Protons and Electrons in Silicon Diffused-Junction Detectors," IEEE Trans. Nucl. Sci. NS-11, No. 3, 206 (1964).

13. Mann, H. M., "Heavy Particle Radiation Damage Effects in Lithium Drifted Silicon Detectors," IEEE Trans. Nucl. Sci. NS-11, No. 3, 200 (1964).

14. Smirnova, I. V., Chapnin, V. A. and Vavilov, V. S., "Radiation Defects in Lithium-Doped Silicon," Soviet Phys. Solid State 4, 2469 (1963).

15. Billington, D. S. and Crawford, J. H., Radiation Damage in Solids, Princeton Univ. Press, Princeton, 1961.

16. Reiss, H., Fuller, C. S. and Morin, F. J., "Chemical Interactions Among Defects in Germanium and Silicon," Bell Sys. Tech. J. 35, 535 (1956).

17. Logan, R. A., "Precipitation of Copper in Germanium," Phys. Rev. 100, 615 (1955).

18. Dash, W. C., "Copper Precipitation on Dislocations in Silicon," J. Appl. Phys. 27, 1193 (1956).

19. Frank, F. C. and Turnbull, D., "Mechanism of Diffusion of Copper in Germanium," Phys. Rev. 104, 617 (1956).

20. Tweet, A. G., "Precipitation of Cu in Ge," Phys. Rev. 106, 221 (1957).

21. Penning, P., "Annealing of Germanium Supersaturated with Nickel," Phys. Rev. 102, 1414 (1956).

22. Tyler, W. W. and Dash, W. C., "Dislocation Arrays in Germanium," J. Appl. Phys. 28, 1221 (1957).

23. Morin, F. J. and Reiss, H., "Precipitation of Lithium in Germanium," J. Phys. Chem. Solids 3, 196 (1957).

24. Dienes, G. J. and Vineyard, G. H., Radiation Effects in Solids, Interscience, London, 1957.

25. Lomer, W. M., "Diffusion Coefficients of Copper Under Fast Neutron Irradiation," AERE Report No. 1540, 1954.

26. Valilov, V. S. and Smirnova, I. V., "Interaction of Lithium Ions Introduced into Silicon with Radiation Defects of the Structure," Soviet Phys. Solid State 4, 830 (1962).

27. Vavilov, V. S., Krukova, I. V. and Chukichev, M. V., "Effect of Lithium on Recombination in n-Type Silicon Irradiated by Fast Electrons," Soviet Phys. Solid State 6, 2097 (1965).

28. Fuller, C. S. and Severiens, J. C., "Mobility of Impurity Ions in Germanium and Silicon," Phys. Rev. 96, 21 (1954).

29. Pell, E. M., "Diffusion Rate of Li in Si at Low Temperatures," Phys. Rev. 119, 1222 (1960).

Chapter II:

1. Taylor, H. S. and Taylor, H. A., Elementary Physical Chemistry, Van Nostrand, New York, 1937.

2. Bjerrum, N., Kgl. Danske Videnskab. Selskab. 7, No. 9 (1926).

3. Fuoss, R. M., "Distribution of Ions in Electrolytic Solutions," Trans. Faraday Soc. 30, 967 (1934).

4. Reiss, H., Fuller, C. S. and Morin, F. J., "Chemical Interactions Among Defects in Germanium and Silicon," Bell Sys. Tech. J. 35, 535 (1956).

5. Smirnova, I. V., Chapnin, V. A. and Vavilov, V. S., "Radiation Defects in Lithium-Doped Silicon," Soviet Phys. Solid State 4, 2469 (1963).

6. Lehrer, F. A. and Reiss, H., "Details of Ion Drift in an n-p Junction," J. Appl. Phys. 33, 2353 (1962).

7. Carslaw, H. S. and Jaeger, J. C., Conduction of Heat in Solids, Oxford Univ. Press, London, 1959, 2nd ed.

8. Pell, E. M., "Ion Drift in an n-p Junction," J. Appl. Phys. 31, 291 (1960).

Chapter III:

1. Miller, G. L., Brookhaven Nat. Lab., Per. Comm.

2. Sullivan, M. V. and Eigler, J. H., "Electroless Nickel Plating for Making Ohmic Contacts to Silicon," J. Electrochem. Soc. 104, 226 (1957).

3. Gyorey, G. L., Thermal Neutron Flux Measurements in a Nuclear Reactor Using Activation Techniques, unpublished, Univ. of Michigan (1963).

Chapter IV:

1. Prince, M. B., "Drift Mobilities in Semiconductors. II. Silicon," Phys. Rev. 93, 1204 (1954).

2. Maira, J. P., "Ion Pairing in Silicon," J. Phys. Chem. Solids 4, 68 (1960).

3. Pell, E. M., "Effect of Li-B Ion Pairing on Li^+ Ion Drift in Si," J. Appl. Phys. 31, 1675 (1960).

4. Cleland, J. W. and Crawford, J. H., unpubl. data quoted in Progress in Semiconductors, edited by A. F. Gibson, P. Aigrain and R. E. Burgess, Heywood and Co., London, 1957, Vol. 2.

5. Price, W. J., Nuclear Radiation Detection, McGraw Hill, New York, 1958.

6. Westinghouse Elec. Corp. Periodic Chart with Nuclear Data (1963).

7. Leibfried, G., "Radiation Damage Theory," paper in Proceedings of the International School of Phys. Enrico Fermi, Course XVIII, Rad. Damage in Solids, Academic Press, New York, 1962.

8. Dienes, G. J. and Vineyard, G. H., Radiation Effects in Solids, Interscience, London, 1957.

Chapter V:

1. Pell, E. M., "Diffusion Rate of Li in Si at Low Temperatures," Phys. Rev. 119, 1222 (1960).

2. Fuller, C. S. and Severiens, J. C., "Mobility of Impurity Ions in Germanium and Silicon," Phys. Rev. 96, 21 (1954).

3. Wertheim, G., "Electron Bombardment Damage in Silicon," Phys. Rev. 110, 1272 (1958).

4. Mann, H. M., "Heavy Particle Radiation Damage Effects in Lithium Drifted Silicon Detectors," IEEE Trans. Nucl. Sci. NS-11, No. 3, 200 (1964).

Appendix A:

1. Kikuchi, C., "Introduction to Semiconductors," in Semiconductor Theory and Technology, Vol. 1, edited by D. Mason, Univ. of Mich. Summer Conf., Summer, 1964.

Appendix B:

1. Reiss, H., Fuller, C. S. and Morin, F. J., "Chemical Interactions Among Defects in Germanium and Silicon," Bell Sys. Tech. J. 35, 535 (1956).

2. Boltaks, B. I., Diffusion in Semiconductors, Academic Press, New York, 1963.